Field-Portable SWIR Acquisition, QA-QC, and Processing Guide

First Edition

McLean Trott[1,2], Collette Pilsworth[1], Stephanie Sykora[4], Nicholas Jansen[5], Matthew Leybourne[1,3], Daniel Layton-Matthews[1], Jon Huntington[6]

[1]Department of Geological Sciences and Geological Engineering, Queen's University, 36 Union Street, Kingston, Ontario, Canada, K7L 3N6
[2]GoldSpot Discoveries Corp.,64 Yonge Street, Suite 1010, Toronto, Ontario, Canada, M5B 1S8
[3]Arthur B. McDonald Canadian Astroparticle Physics Research Institute, Department of Physics, Engineering Physics & Astronomy, Queen's University, Kingston, Ontario, Canada K7L 3N6
[4]OreQuest Consultants, 6891 Wiltshire St., Vancouver, BC, Canada, V6P 5H2
[5]Teck Resources Limited, Bentall 5, 550 Burrard St #3300, Vancouver, BC V6C 0B3
[6]HH Geoscience, 34 Craiglands Ave., Gordon, NSW 2072, Australia

2022

TABLE OF CONTENTS

Figures

Tables

Field-Portable SWIR Acquisition, QA-QC, and Processing Walkthrough

First Edition

McLean Trott[1,2], Collette Pilsworth[1], Stephanie Sykora[4], Nicholas Jansen[5], Matthew Leybourne[1,3], Daniel Layton-Matthews[1]

[1]*Department of Geological Sciences and Geological Engineering, Queen's University, 36 Union Street, Kingston, Ontario, Canada, K7L 3N6*
[2]*GoldSpot Discoveries Corp.,64 Yonge Street, Suite 1010, Toronto, Ontario, Canada, M5B 1S8*
[3]*Arthur B. McDonald Canadian Astroparticle Physics Research Institute, Department of Physics, Engineering Physics & Astronomy, Queen's University, Kingston, Ontario, Canada K7L 3N6*
[4]*OreQuest Consultants, 6891 Wiltshire St., Vancouver, BC, Canada, V6P 5H2*
[5]*Teck Resources Limited, Bentall 5, 550 Burrard St #3300, Vancouver, BC V6C 0B3*

ABSTRACT

Short wave infrared (SWIR) data derived from field-portable or benchtop hardware can provide useful vectors for mineral exploration. Acquisition of data with suitable QA-QC measures in place, capture of relevant metadata, database storage of raw data and processed results, and processing itself can be a barrier to uptake for new users and problematic for fusion of datasets even when this data is acquired by experienced practitioners. The intention of this walkthrough is to mitigate these issues by providing explicit and detailed guidance on these aspects of SWIR spectroscopy in the form of a practical workflow and attached templates and supplementary materials.

It is our hope that adoption of protocols derived from this document will facilitate a greater conversation in academia and industry around the capture, storage, and interpretation of this sort of data, and lead to ever-improving data and interpretive quality for current and future practitioners to apply to mineral exploration or rock characterization problems.

1. INTRODUCTION

1.1 Objectives

Welcome to the exciting world of (field portable) short-wave infrared (SWIR) and visible to near infrared (VNIR) spectroscopy! Presumably you're reading this for one of two reasons:

1) You're a practitioner and are interested in implementing/contributing to establishment of standards and best practices for this technique.

2) You're new to this and would like to get started.

Either way you are in the right place.

This document and appendices are intended to provide a public domain guide for practitioners (perhaps in the mineral exploration industry, academia, or another field) to work toward standardizing the acquisition, storage, and interpretation of spectral datasets. It's also intended to

be accessible to newcomers and provide step-by-step instruction. This is a first edition; readers are invited to submit suggestions to the authors for addition to future editions.

1.2 The electromagnetic spectrum: starting at the start

The electromagnetic spectrum (Figure 1) refers to the broad range of wavelengths of electromagnetic energy in the known universe, from long wavelength radio waves all the way down to short wavelength gamma waves.

As human beings, our eyes register a small segment of this range, visible light (390 to 750 nm). Your food is heated in a microwave oven by another small segment. AM/FM radios pick up signals from another segment. Much of the technology around us is related to signals or energy transmitted and received using certain portions of the spectrum.

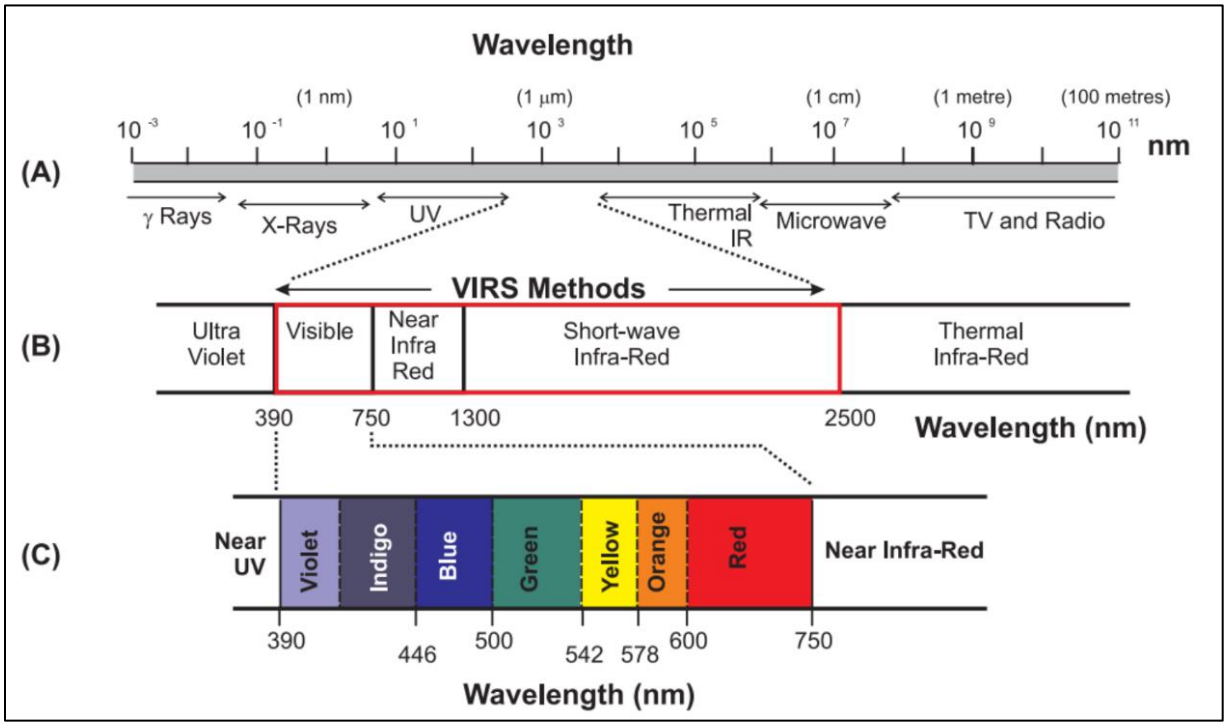

Figure 1) From (Kerr et al., 2011) after (Hauff, 2008). The electromagnetic spectrum. showing the regions of interest for SWIR and VNIR spectroscopy.

1.3 SWIR spectroscopy: what is it?

The method examines a range of the electromagnetic spectrum from approximately 1300 – 2600 nm, recently described as SWIR 1 (1300 – 1850 nm) and SWIR 2 (1850 – 2600 nm), differentiated by their vibrational modes (Laukamp et al., 2021). SWIR 2 extends to 2600 nm but most instrumentation reaches 2500 nm only. Certain bonds, primarily those involving oxygen or ammonium, vibrate when impacted by energy at specific wavelengths within this range, converting some of the incident energy into kinetic energy and therefore reflecting a modified spectrum with lower intensity at the corresponding wavelength (Figure 2 and Table 1). In practical terms, this means shining a light on a sample, capturing the reflected spectra, and processing it such that the absorption features reveal the composition of the sample by relating

the geometry of absorption features to a specific SWIR-active mineral or combination of such minerals.

The scale of application, discussed herein focuses on spectra collected with field-portable instrumentation such as Spectral Evolution's oreXpress or Malvern Panalytical's ASD Terraspec models. Instruments like these typically expose a sample to a light source through a window of approximately 2 cm diameter (this varies by model and probe attachments), and then route the reflected light back to sensors and a processing unit to capture a spectrum. Spectra are ultimately downloaded from the unit and processed with a software to assign mineral matches through comparison with a library of reference spectra, and to extract geometric or spectral shape information for relevant absorption features, such as the width (or full width half maximum; FWHM), depth (D), and wavelength at minimum (W), as shown in Figure 2. These numeric representations of spectral geometry are referred to collectively as *parameters* or individually as *scalars* or *indices*.

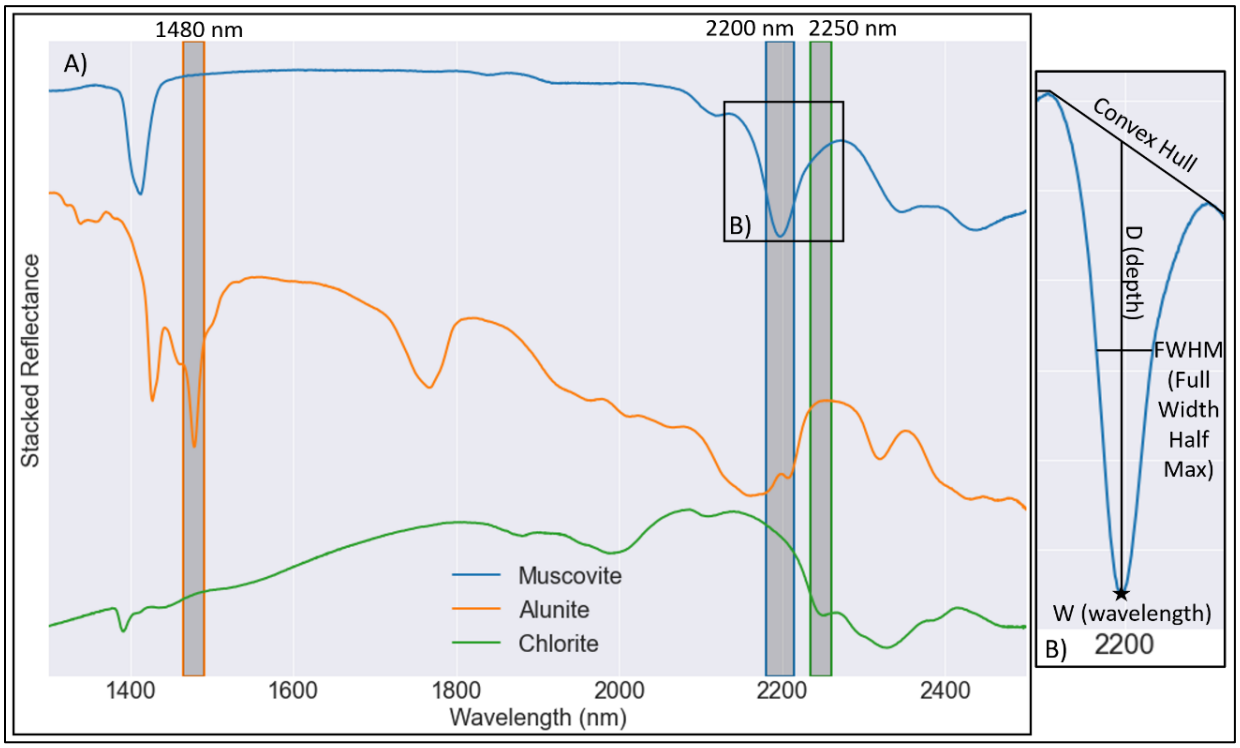

Figure 2) From (Trott et al., 2022). Examples of SWIR spectra extracted from the JPL Ecostress spectral library (Grove et al., 1992), showing key absorptions for the three minerals discussed as vectors. B) Insert illustrates the nomenclature of absorption feature scalars applied to the 2200nm "AlOH" absorption for muscovite. The exact value of the wavelength in nanometers at its minimum is represented by W. Depth (D) is measured from the base of the absorption (the minimum) vertically to where it intercepts the Convex Hull line, formed by connecting apices along the spectral curve. FWHM is measured at the midpoint of D, between either side of the absorption.

SWIR sensing technology is applied at various other scales in the mineral exploration industry. Satellite multispectral systems such as Landsat and ASTER apply the same principles, although at much coarser wavelength and spatial resolutions. In areas of abundant outcrop these satellite-borne methods may be useful for identifying the geometry of large alteration zonation patterns or systematic variations in mineral chemistry (Bedell et al., 2009). At an intermediate scale,

airborne hyperspectral systems (e.g., HyMap) may be applied for greater spatial and spectral resolution than satellite systems, and broader coverage than handheld systems (Cudahy et al., 2001). In many cases, handheld methods and airborne or satellite systems are used in conjunction, whereby handheld measurements contextualize results by constraining the spectral response of representative samples from a larger area of study (Lampinen et al., 2017).

In recent years SWIR acquisition has been applied using core scanning techniques, in essence producing a spatially related string of spectra (e.g., HyLogger) or a spectra per 'pixel' as opposed to localized point readings (e.g., CoreScan or Terracore platforms). These instruments provide exponentially more information but may come with some drawbacks. Some of them, particularly those with a high resolution, tend to be large and costly to mobilize and operate, and produce heavy datasets (on the order of terabytes) which may be unwieldy to process and interpret without highly specialized knowledge about SWIR methods AND access to cloud or cluster computing.

Position (nm)	Mechanism	Mineral Group	Mineral examples	Comments
1400	OH/H_2O	Clays, sulfates, hydroxides, zeolites	kandite, smectite, jarosite, alunite, gibbsite	
1485	OH/H_2O	Sulfates, sheet silicates	alunite, prehnite	Very specific to alunite.
1550	NH_4, Fe/Mg-OH	Ammonia-bearing species, sorosilicates	alunite-NH3, buddingtonite, epidote, clinozoisite	
1760	OH/H_2O or S-O	Sulfates	gypsum, alunite	
1850	OH and water	Sulfates	jarosite	
1900	Water	Smectites	palygorskite, nontronite, montmorillonite	
2020 - 2120	NH_4	Ammonia-bearing species	alunite, smectite, buddingtonite, white mica	
2160	OH/H_2O	Di-oct. sheet silicates	kandite, pyrophyllite	
2200	Al-OH	Di-oct. sheet silicates, cyclosilicates, sulfates	kandite, white mica, tourmaline, jarosite, prehnite	Perhaps most relevant to vectoring with white mica spectra.
2250	Fe/Mg-OH	Tri-oct. sheet silicates, sorosilicates, cyclosilicates, sulfates, hydroxides	biotite, phlogopite, epidote, tourmaline, jarosite, gibbsite	Perhaps most relevant to vectoring with chlorite spectra.
2290	Mg-OH	Talc, tri-oct. sheet silicates, cyclosilicates, Ca-amphibole	talc, smectite, tourmaline, tremolite-actinolite	
2320	CO_3	Carbonates	calcite, dolomite, siderite, ankerite, magnesite	The feature used for identification of carbonates, although overlap with 2340 can complicate this. Access to the 2505-2541 carbonate absorption would mitigate this but is not generally available.
2340	Mg/Fe-OH	Chlorites, di-oct. sheet silicates, tri-oct sheet silicates, sorosilicates	chlorite, white mica, biotite, phlogopite, epidote	Complementary to 2250nm absorption although generally not as well developed.
2390	Mg/Fe-OH	Tri-oct. sheet silicates, talc, Ca-amphibole	biotite, phlogopite, talc, tremolite-actinolte	Complementary to 2250nm absorption although generally not as well developed.
2505-2541	CO_3	Carbonates	calcite, dolomite, siderite, ankerite, magnesite	Beyond the range of most commercially available instruments.

Table 1) Modified from (Hauff, 2008; Laukamp et al., 2021). Major absorption features in the SWIR range. Absorption of energy occurs at these wavelength positions depending on the presence of the bonds listed under "Mechanism".

1.4 Absorption Geometry and Scalars

A spectrum consists of numerous 'bands' of relative reflectance/absorbance information. A spectrum not only facilitates mineral identification, but also quantifies often overlooked spectral characteristics such as absorption feature position, width, and depth, as shown in Figure 2, and ultimately mineral compositions. Software is used to extract and numerically represent these features in a semi-automated fashion. Each scalar extracts a single predefined feature from the spectrum in question, or calculates a value based on other scalar outputs. An extracted scalar

value numerically represents some mineralogical aspect of the sample. Although several software solutions for this purpose are available, this document is focused on usage of The Spectral Geologist (TSG), described further in Section 5.2.

The relative depths (in reflectance %) of absorption features (D-prefixed scalars) are measured vertically from the minimum point up to where it intercepts a background, or Convex Hull, as shown in Figure 2 inset B. The convex hull is a reference line (may be thought of as a piece of string draped across a spectrum) made by fitting a downward concave curve to the overall trend of the un-normalized spectral peaks on either side of an absorption feature. From this the Hull Quotient (HQ) curve (or a normalized version of our spectrum) is calculated by dividing the original reflectance by the convex hull. In other words, the depth of an absorption feature needs to be measured against a 'roof' and the HQ curve is a broadly accepted means of assigning that roof consistently. The width of an absorption (or Full Width Half Maximum, FWHM-prefix) is the length (in nm) of an imaginary perpendicular line across the center of the D line (Figure 2). The wavelength position (W-prefixed scalars) identifies the wavelength of the bottom of a given absorption feature. These W-scalars are frequently of use for vectoring to ore deposits as in many cases changes in the wavelength at minimum are the result of systematic changes in the substitution chemistry of a given mineral group, which may be a proxy for distance from source. For example, the three absorption feature wavelengths for alunite, white mica, and chlorite, shown in Figure 3 capture the changes of W1485, W2200, and W2250 as proxies for their composition, and show zonation with regards to porphyry copper deposit geometry in many cases.

2. SWIR TECHNIQUES IN MINERAL EXPLORATION

2.1 Section Introduction

Short-wave infrared techniques are increasingly applied in mineral exploration, particularly for hydrothermal deposit types where alteration mineral zonation is well developed (Hauff, 2008), but difficult to visually recognize (e.g., abundant white, fine-grained mineral species). Alteration minerals in these scenarios commonly contain oxygen in water or hydroxyl bonds and as a result are SWIR-active (Duke, 1994), meaning easily identified through examination of their spectral response. Subtle variations in the chemistry of some of these minerals may be examined spatially through changes in the position of absorption feature wavelengths for a given species, which may be related to distance from source. Both potential vector types, alteration mineral distribution and mineral chemistry variation, can be difficult to identify visually (Crósta, 1990). A third vector type, undetectable to the human eye, involves calculations performed on multiple absorption features to proxy the degree of crystallinity of mineral families such as white micas or kaolinite. These values indicate the relative temperature of formation of the relevant mineral group, and when viewed spatially may provide a proxy for distance from source. An example of this, the 'white mica crystallinity' scalar, is shown in Figure 3.

Deployment of portable SWIR acquisition hardware mitigates the wavelength limitations of the human eye, enabling rapid and cheap data acquisition to identify these zonation patterns in alteration assemblages and mineral chemistry variation.

2.2 Vector Types

2.2.3 Alteration Mineral Distribution

Zonation patterns of alteration minerals with respect to hydrothermal deposit types are generally well established. These patterns may be visible upon visual inspection but subtleties in alteration facies are often more difficult to differentiate, particularly in so-called “white rock” alteration zones such as the advanced argillic and phyllic (a.k.a. sericitic) zones of a porphyry copper system. In the case of the advanced argillic assemblage, the distribution of white, often fine-grained clay or sulphate minerals such as kaolinite, alunite, dickite, diaspore, or pyrophyllite has distinct implications in terms of pH and temperature of formation and by proxy, relative distance to source. These minerals are difficult to differentiate visually but are easily identified using SWIR methods. In Figure 3 we can see the broad geometric relationships between porphyry copper alteration assemblages and their SWIR-active mineral assemblages.

Examining SWIR mineral matches for systematically collected data on drill-cores in 3D may prove vital in identifying the placement and context of alteration assemblages and therefore provide indications of the location of mineralization, informing further drilling.

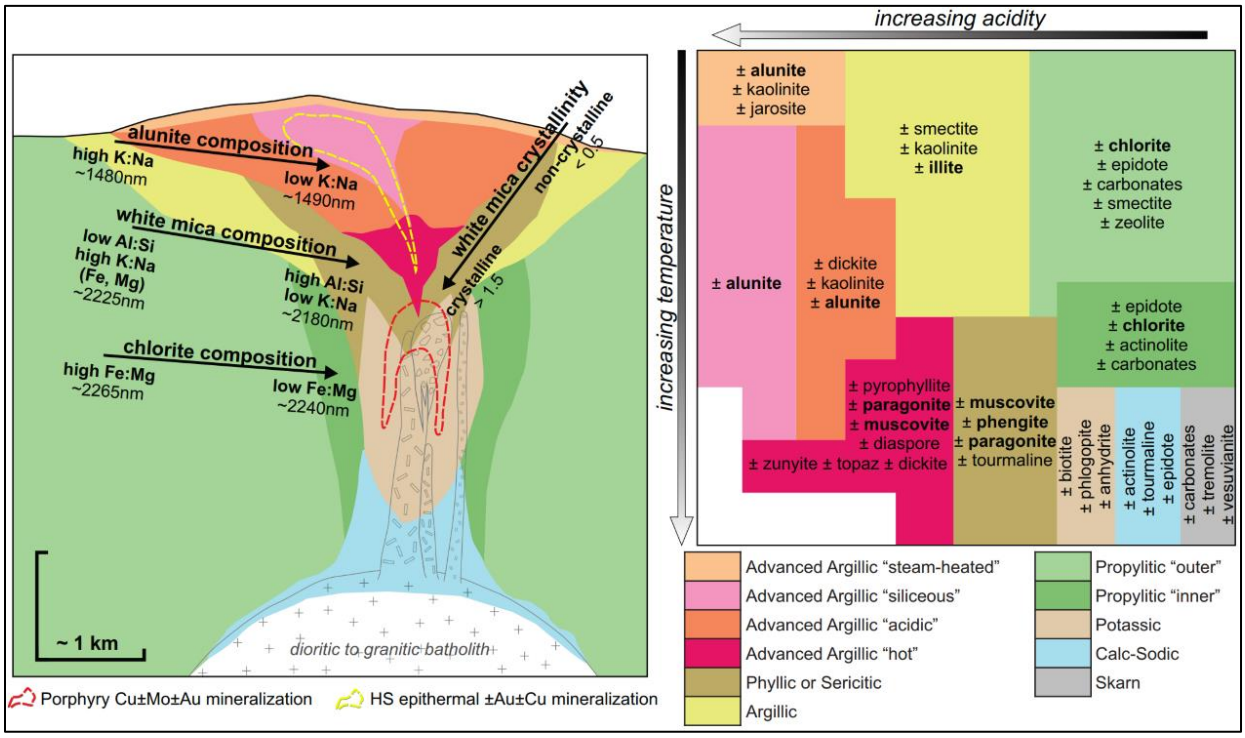

Figure 3) From (Trott et al., 2022), modified from (Corbett and Leach, 1998; Halley et al., 2015). Generalized porphyry copper alteration model (calc-alkalic Cu-Au "A-vein" type) showing distribution of alteration zones and their corresponding SWIR-active minerals.

2.2.4 Mineral Chemistry Variation

The substitution chemistry of some mineral types may be examined through its spectral response. Tschermak-type substitution where Al is replaced by (Fe, Mg) + Si in white mica minerals (i.e., illite, phengite, paragonite, muscovite) can be captured by examination of the wavelength at minimum (W2200) of the “AlOH” 2200 nm absorption feature (Duke, 1994; Halley et al., 2015;

Scott and Yang, 1997; Swayze et al., 1992). This substitution is controlled by factors like pH and concentrations of Fe2+ and K+ in the hydrothermal fluid (Halley et al., 2015) as it reacts with country rock and precipitates white mica minerals during the formation of phyllic or sericitic alteration assemblages in a porphyry system. More specifically, the value of W2200 shifts from 2180 to 2225 nm as white micas increasingly substitute (Fe, Mg) + Si for Al, transitioning from paragonitic to phengitic composition.

Another potential SWIR vector involves estimation of the Mg# for chlorite-dominated spectra, observed in the Fe:Mg ratio and seen in a wavelength shift of the "Fe/MgOH" absorption feature found around 2250 nm (W2250), and strongly coupled with a wavelength shift in the "Mg/FeOH" absorption feature around 2340 nm (W2340) (Neal et al., 2018; Scott et al., 1998). Higher 2250W values indicate higher Fe relative to Mg, and vice versa (Jones et al., 2005; Lampinen et al., 2017). In settings containing abundant hydrothermal alunite, the shift in an absorption feature around 1480 nm may be used to indicate the Na:K ratio, where higher/longer wavelengths indicate an increase in this proportion corresponding to a higher temperature of formation, and by proxy, nearness to source (Chang et al., 2011).

The application of a given vectoring method is highly dependent on the scenario; white mica chemistry is likely to be very useful where widespread sericitic alteration is outcropping or has been drilled, chlorite mineral chemistry is likely to be useful in a propylitic-type environment, and alunite mineral chemistry may prove useful in the lithocap, or advanced argillic environment. Figure 4 illustrates the distinct environments where white mica vectors may be favored as opposed to alunite vectors. Figure 6, from Lampinen et al. (2017), also summaries some of the commonly used scalars mentioned herein.

2.2.5 Crystallinity Vectors

The crystallinity of white micas, as seen in Figure 3 and the center panel of Figure 4, can be estimated by division of the "AlOH" feature depth (D2200) by the depth of the water absorption feature found at 1900 nm (D1900) (Medina et al., 2021). Under higher temperatures of formation, white micas tend to crystallize with a more orderly structure and as a result incorporate less water in interlayered smectites, proxied by the relative depths (spectral abundances) captured by scalars for the D2200 white mica and D1900 water features.

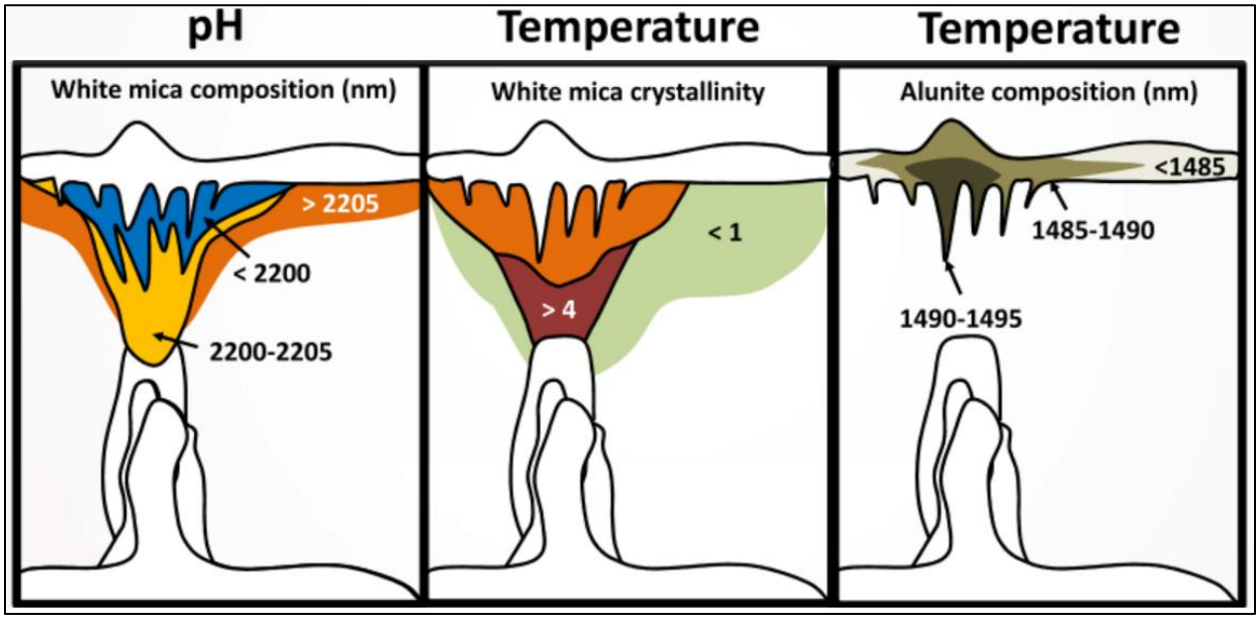

Figure 4) From (Jansen and Trott, 2018). Some commonly used vectors for porphyry copper exploration using mineral chemistry (white mica composition W2200 and alunite composition W1485), and crystallinity (white mica crystallinity).

MFEM scalar name	Plain description	Base algorithm/references/scalar aliases
Al-OH feature depth	Relative depth of the Al-OH feature at 2,200-nm wavelength indicative for Al-OH-bearing mineral abundance	Relative depth of the 2,200-nm wavelength absorption for which the continuum is removed between 2,120 and 2,245, determined using a 3-band polynomial fit around the band with the lowest reflectance, "D2200"
Al-OH feature shift	Shift of the Al-OH feature caused by Tschermak's substitution of Al in white micas	Minimum wavelength of the 2,200-nm absorption for which the continuum is removed between 2,120 and 2,245, determined using a 3-band polynomial fit around the band with the lowest reflectance,"W2200"
Kaolin group index <1.005: no kaolin >1.005: kaolin	Intensity of the 2,160-nm feature, indicative for kaolinite abundance used in separating kaolin group from other minerals having Al-OH feature at 2,200 nm such as Al smectites and white mica	(R2136 + R2188)/(R2153 + 2171), Haest et al. (2012a, b) "2160D2190"
Kaolin group crystallinity Low: poorly ordered High: well ordered	Crystallinity of kaolin group minerals (kaolinite, halloysite, dickite, and nacrite) ranging from well to poorly ordered kaolinite	[(R2138 + R2173)/R2156]/[(R2156 + R2190)/R2173] Based on Sonntag et al. (2012) "Kaolin composition index"
Fe-OH feature depth	Relative depth of the Fe-OH feature at 2,250 nm wavelength; indicative for Fe-OH mineral abundance	Relative absorption depth of the 2,250-nm absorption for which the continuum is removed between 2,230 and 2,280, determined using a 3-band polynomial fit around the band with the lowest reflectance, "2250D"
Fe-OH feature shift 2,248 nm: Mg rich 2,261 nm: Fe rich Bishop et al. (2008)	Estimation of the Mg/Fe ratio in chlorite, but also the shift of a coinciding absorption feature in epidote and biotite, where the wavelength position is not necessarily only due to the Mg but possibly more due to the relative Al, Fe^{3+} or Ca content	Minimum wavelength of the 2,250-nm absorption for which the continuum is removed between 2,230 and 2,280, determined using a 3-band polynomial fit around the band with the lowest reflectance, "W2250"
Mg-OH feature depth <1.025: Al smectite >1.035: white mica Haest et al. (2012a, b)	Depth of 2,350-nm feature, evident in white mica; used to separate white micas from Al smectites, when Al-OH feature is present, carbonate minerals can be separated from white micas and chlorites based on their left symmetry (Gaffey, 1987)	(R2326 + R2359)/(R2343 + R2359), Haest et al. (2012a, b), "2350De"

Figure 5) From (Lampinen et al., 2017). Descriptions of some scalars commonly used for vectoring. It should be noted that TSG base scripts using the profile method and 3- or 5-point polynomial fitting may generate artefacts. Instead, the "Pfit" method is suggested.

3. QUALITY CONTROL AND QUALITY ASSESSMENT

3.1 Section Introduction

Consistent data collection with QA-QC controls is critical, especially for large projects with multiple users, over a long period, and potentially with multiple instruments. Wavelength differences of up to 5 nm for W1480 (alunite-related) and 2 nm for W2200 for the same samples analyzed using different instruments have been documented (Chang and Yang, 2012; Uribe-Mogollon and Maher, 2020). Proper standardization allows for robust interpretation and facilitates application of machine learning techniques, which tend to require 'apples-to-apples' feature inputs. The need for guidelines and standards in this space has been highlighted previously (Kerr et al., 2011).

Ideally, the analysis should be conducted in an environment with consistent lighting, however, good contact between the instrument and rock surface should minimize noise related to fluctuations in variable lighting conditions (Trott et al., unpublished). Analysis can be applied to uneven, flat, or rounded (e.g., drill core) rock surfaces. Rock chips (1 to 5 mm; e.g., reverse circulation chips) provide the best medium for sample representativity; fine pulps generate noisy spectra and should not be used. Spectra can be captured for residual soils, sieved to a standard size (e.g., -80 mesh), and may be particularly useful combined with soil geochemistry data.

A critical requirement is that the sample is dry, as H2O is spectrally active. Samples can be dried in a sunny area or in an oven at temperatures less than ~40° C, as higher temperatures could change the structure of some clays (e.g., convert smectite to illite) (Russell and Farmer, 1964).

3.2 QA-QC Measures

The first mandatory QAQC measure for SWIR spectrometers includes measuring a Spectralon™ white reference disc comprised of a fluoropolymer with nearly 100% reflectance in the SWIR range (Bruegge et al., 1993) If the various sensors in the instrument are functioning properly and the instrument is calibrated it will produce a flat line spectrum. The Spectralon™ disc can also act as a 'blank' to determine if there is any dust or debris in the analytical probe. Most instruments are shipped with at least one Spectralon™ white reference disc. Care must be taken to keep them clean and not touch the upper surface, as skin oils can contaminate the spectral response. Contaminated discs can be recovered by wet sanding the surface with fine carbide sandpaper and allowing it to dry overnight.

A second mandatory QAQC measure is the analysis of a Mylar 'standard', which has five pronounced absorptions (1128.7, 1660.1, 1952.9, 2131.6, and 2256.0 nm) allowing the user to determine the accuracy of their instrument and whether it is within calibration limitations (i.e., within ± 1 nm of the known absorption feature wavelength). The ideal method for analyzing the Mylar standard is by placing it on top of the Spectralon™ disc.

We also recommend usage of an in-house standard consisting of a mineral with a relatively homogeneous composition, which occurs in the study area; ideal candidates might be white mica (illite, paragonite, muscovite, phengite), kandite (halloysite, kaolinite, nacrite, dickite), alunite, and/or a chlorite-rich sample. The Mylar and in-house standards allow the user to track accuracy and variation in key absorptions features (e.g., W2200, W1480, etc.) over time and between instruments, allowing results to be leveled, if necessary.

Analytical duplicates (duplication of an analysis spot) are also recommended to ascertain the precision of results.

All four of these QAQC measures should be used at the beginning and end of the analysis session and periodically (intervals of ~ 20 measurements) throughout the session.

3.3 QAQC Evaluation

Two basic plots can be used to assess quality of collected data. A first pass assessment of spectral quality may be carried out using a plot of Signal to Noise against Error (Figure 7.A). It must be kept in mind that rocks containing minimal amounts of SWIR-active minerals may also plot in the "Poor quality" field. For this reason, some caution must be applied during the evaluation process, and it may not be advisable to reject a spectrum based on this plot alone. A bound water vs unbound water plot, as shown in Figure 7.B, can indicate if wet samples may have negatively impacted the quality of spectra acquired.

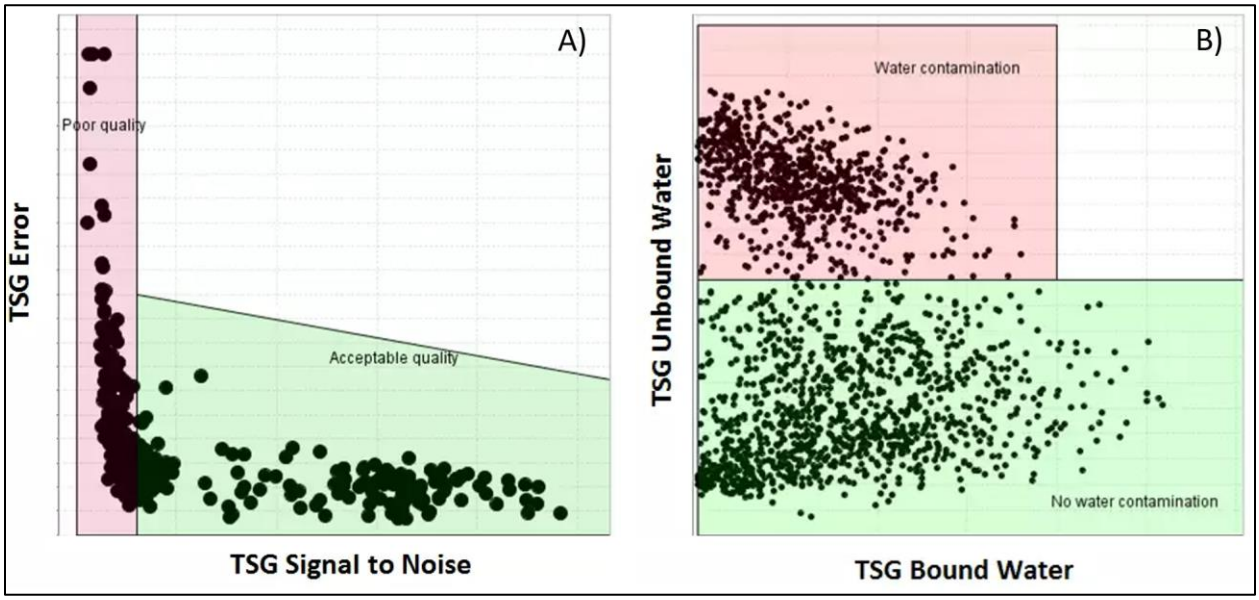

Figure 6) Quality assessment based on Signal to Noise ratio versus Error (A), and assessment of water interference based on the amount of unbound water relative to bound water (B). Plots generated in ioGAS.

To create a similar pair of plots in TSG8, navigate to the "Scatter" view and customize the X and Y fields found at the base of the upper toolbar (Figure 7).

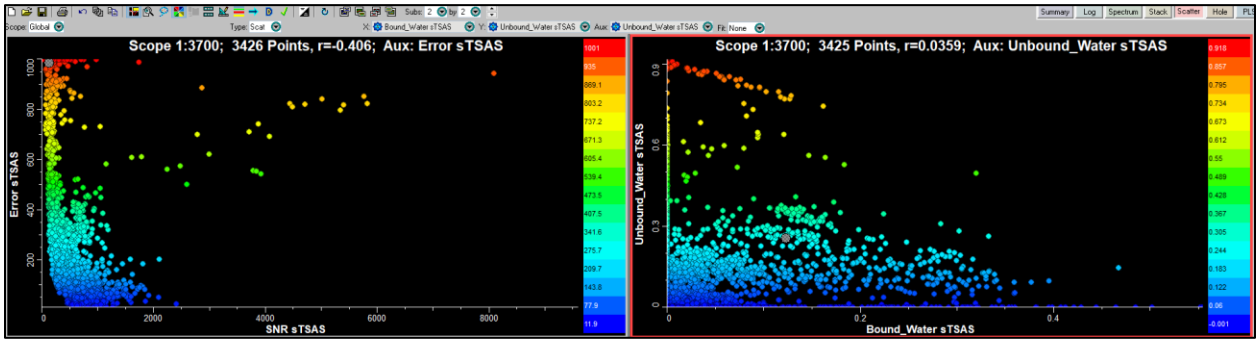

Figure 7) Plots for evaluation of spectral quality and wet samples (SNR = Signal to Noise Ratio). Plots generated in TSG.

Assessment for instrument drift or acquisition problems can be carried out after collection is complete and the "Mylar_QAQC_scalars.tsg" template file has been applied to the data. Return to this after proceeding through Sections 4 and 5. The fundamentals of preparing the Mylar QA-QC data are basically the same, except the mylar tsg template is applied instead of the SWIR template, and the exported scalars can be filtered down to the readings taken on Mylar.

The "Mylar_QAQC_scalars.tsg" template will extract the wavelength position of the four prominent Mylar absorptions, 1660.1, 1952.9, 2131.6, and 2256.0 nm, respectively. Four additional scalars, prefixed with "Diff" are used to calculate the difference between the ideal position and the measured position. These four scalars should be plotted and examined for differences of greater than 1 nm (positive or negative). The example shown in Figure 8 is drawn from Mylar readings taken using the same instrument on the same sheet of Mylar throughout an acquisition session, and show very consistent results, mainly within tolerance (± 1 nm of the

idealized absorption). Results plotting outside of this tolerance range require follow-up to assess if the measurements taken during those sessions are valid, require correction, or must be discarded.

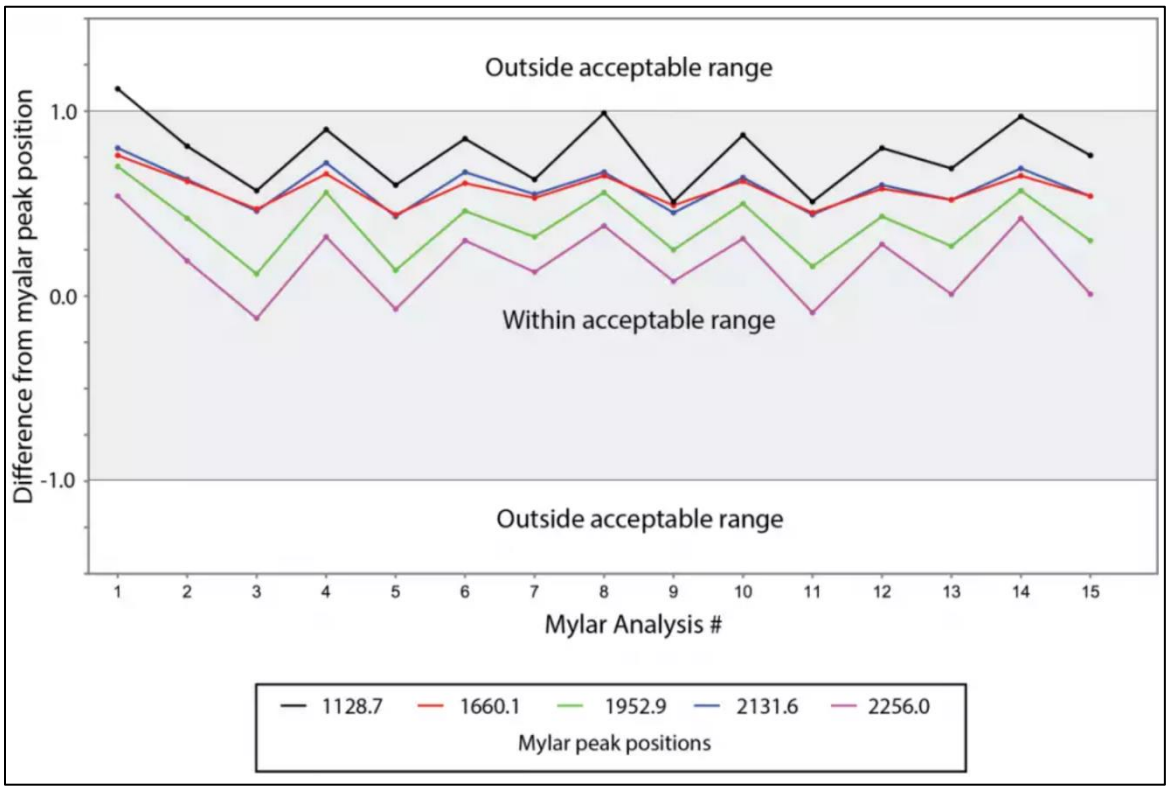

Figure 8) Mylar QA-QC assessment visualized in sequence of acquisition through an analytical session. From (Jansen, 2016).

4. ACQUISITION

4.1 Section Introduction

Since the introduction of the PIMA by Integrated Spectronics (Thompson et al., 1999), numerous manufacturers have developed a wide range of field-portable instruments with varying characteristics and distinct acquisition software to accompany them. This information should be laid out in the user's guide accompanying the make and model in use. Manufacturer's instructions should be followed carefully during acquisition.

QA-QC measures, as described above, should be inserted in the sample stream, and metadata, as described below, should be carefully recorded at the time of capture, and saved into a stable, accessible database for future use.

4.2 Metadata Capture

Regardless of manufacturer and instrument specifics, some critical information must be recorded at the time of acquisition, for two important purposes: 1) to facilitate QAQC evaluation, and 2) to relate results to their geographic location.

Key metadata that should be recorded at the time of collection are Spectral ID, user, date, instrument model, instrument serial number, analysis time, location (depth and drillhole ID for

subsurface data, or X (easting/longitude) and Y (northing/latitude) coordinates and corresponding datum for surface data), and sample medium (e.g., rock, drill core, rock chips, QAQC/type etc.). If readings are being taken on coarse laboratory rejects then the corresponding sample ID should be recorded, so that the results can be easily merged with any corresponding geochemistry later. The above information should be recorded digitally and warehoused in a database where it can be extracted, merged with results, and used to evaluate QAQC and locate the results geographically (i.e., import into a GIS platform or 3D visualization software).

An example of a basic metadata capture sheet implemented in Microsoft® Excel can be found in Appendix A. Cell validation for some data types (i.e., date and time formats, pick lists, etc.) has been applied as per the Format column in Table 2.

Column Header	Description	Format	Examples
SpectralID	*Critical field for relating results from TSG, or raw spectra, to the correct metadata.*	**text*	PROJNAME_000001.asd
Sample_Type	*A.K.A. Sample medium*	**pick-list*	Drill-core, Hand Sample, Outcrop, Coarse Reject, Soil, Sieved, RC Chips
QAQC_Type	*Regular sample or some form of QAQC sample?*	**pick-list*	SAMPLE, DUPLICATE, MYLAR, STD-1, STD-2, SPECTRALON
SampleID	*Use this if reading taken on a coarse reject or soil sample which will also ultimately have geochemical results.*	**text*	LABSAMPLE_01987
HoleID	*If taken on Drill-core*	**cell*	DDH_2022-01
Depth_m	*If taken on drill-core*	**numeric*	230.5
From_m	*If taken on coarse rejects from drillcore (corresponding interval).*	**numeric*	230
To_m	*If taken on coarse rejects from drillcore (corresponding interval).*	**numeric*	232
Easting	*If taken in the field or from a hand sample brought back from this location.*	**numeric*	
Northing	*If taken in the field or from a hand sample brought back from this location.*	**numeric*	
CRS_datum	*coordinate reference system or datum used for Easting/Northings. (field or hand sample)*	**pick-list*	WGS84_N16, WGS84_N15, etc.
Instrument	*Instrument make/model and serial number. To consider differences between machines if multiple machines used.*	**pick-list*	Halo (SERIAL#), OreXplorer (SERIAL#), PIMA (SERIAL#), Hi-Res 4 (SERIAL#), NA (historic data)
Acquisition_Date	*On windows computer CTRL-; (semi-colon)*	**YYYY-MM-DD*	2023-08-22
Acquisition_Time	*On windows computer, CTRL-SHIFT-; (semi-colon)*	**HH_MM_SS*	14:23:00
Acquisition_Location	*In case environmental parameters have an impact on spectral response (I.E. humidity in an outdoor setting)*	**pick-list*	Core Shed "A", Core Shed "B", In Field (see coordinates), in Laboratory "A"
Sample_Type	*Geological context of where the measurement was taken, or if acquisition was simply carried out systematically (ie by geotechnicians).*	**pick-list*	Vein, Vein Halo/ Aureole, Wallrock, Breccia Fragment, Breccia Matrix, Random/ Systematic, Contact Alteration Aureole, Fracture Surface
User	*In case questions arise as to collection methods.*	**pick-list*	Jane Doe, John Doe
Comments	*Any additional information, as needed.*	**text*	Rubbly interval, difficult to find flat surface.

Table 2) Some suggested metadata fields. For a simple example of a metadata spreadsheet with cell validation included see Appendix A: "AppendixA_Spectral_Metadata.xlsx".

5. PROCESSING

5.1 Section Introduction

Historically users needed to specialize extensively in a very manual process of identifying mineral species from individual spectra, a time-consuming endeavor with the quality of results highly dependent on the expertise of the user. A very apt commercial solution to this, aiSIRIS, consists of a cloud-based, largely automated software wherein uploaded spectra are classified relative to a large library of expert-interpreted spectra. Presented results emphasize estimated minerals and scalars, not their input spectra. For users who wish to interpret spectra themselves, in a more involved way, The Spectral Geologist (TSG) software enables bulk processing of large volumes of spectra through its implementation of (i) 'The Spectral Assistant' to unmix spectra against a pure mineral reference library for mineral identification and (ii) extraction of 'scalars' to quantify the geometry (shapes) of key absorption features (Berman et al., 1999; Huntington et al., 1999). TSG is apt for bulk processing tasks but still requires a certain level of prior knowledge to operate effectively and reduce the resulting data into useful vectors. For companies with a great deal of throughput and perhaps multiple sites, aiSIRIS is likely the best alternative, for consistency in processing and comparability (provided that adequate QA-QC measures are implemented during capture). For smaller companies wishing to develop in-house knowledge, academics who desire more control over the processing of their data, or aiSIRIS users wishing to perform their own QA-QC, TSG is a good option. This manual focuses on the second scenario and is intended to guide a novice or experienced user equally through a robust workflow to process spectral datasets. For further information not included in the following workflow, the TSG Manual itself is available in the Help menu within the software (or online, here: https://research.csiro.au/thespectralgeologist/support/downloads/).

This paper is not intended as a replacement for the TSG manual, rather to provide walkthrough-style guidance geared specifically toward processing and cleaning spectral data for mineral exploration.

5.2 The Spectral Geologist

TSG is a software created by Commonwealth Science and Industrial Research Organization (CSIRO), Australia, for unmixing and extracting information from VNIR, SWIR, and thermal infrared (TIR) spectra. It uses an algorithm called 'The Spectral Assistant' (TSA) as default to identify minerals and relative spectral abundances (Huntington et al., 1999; Schodlok et al., 2016). It compares new spectral data against a curated internal spectral library developed and maintained by CSIRO (Smith, 2016), unmixing acquired spectra to their closest equivalents or mixed assemblages in the library. TSG allows for bulk processing of hundreds or even tens of thousands of spectra in a highly repeatable manner, which can be carried out in minutes, not days.

A caveat here is that the current TSA version (V8) will unmix up to four most predominant mineral signatures per spectrum at most. An experienced interpreter would most likely be able to manually extract more minerals from the same spectra but at a much higher time cost.

TSG may be downloaded at https://research.csiro.au/thespectralgeologist/tsg/pricing/, and licensed for blocks of time ranging from 7 days for $110 AUD to 3 years for $4950 AUD (current as of time of this publication).

Installing TSG without an active license will enable it to act as a free (read-only) base version for viewing previously processed results. For users with background in the python programming

language (Van Rossum and Drake Jr, 1995), existing .tsg files can be read and viewed using the "pytsg" library (Chi, 2022) found at https://github.com/FractalGeoAnalytics/pytsg.

5.2.1 Customizing an active minerals list

TSA is a general-purpose unmixing algorithm that, initially, does now know where in the world your spectra come from or the source or style of geological environment. Its first pass then is called a "system" level interpretation of the minerals. The user may then choose to apply some context to the project being addressed (e.g., is it porphyry, epithermal, advanced argillic, orogenic gold, base metal or sedimentary). Armed with this understanding the user may create an "Active Minerals List", or AML, that informs a second TSA iteration leaving out those minerals that are thought to be irrelevant to the expected model, but still allowing some room for serendipity. The "Active Mineral Classes" menu shown in Figure 9 may be accessed via "File->Settings->TSA->Select active minerals". This second TSA iteration (much faster to process than the first iteration) produces a more reliable "User" level interpretation. Both "System" and "User" results should be archived in case a further iteration is required, but for most applications the "System" level interpretation is merely an important part of the recommended workflow to arrive at optimal results and can be set aside.

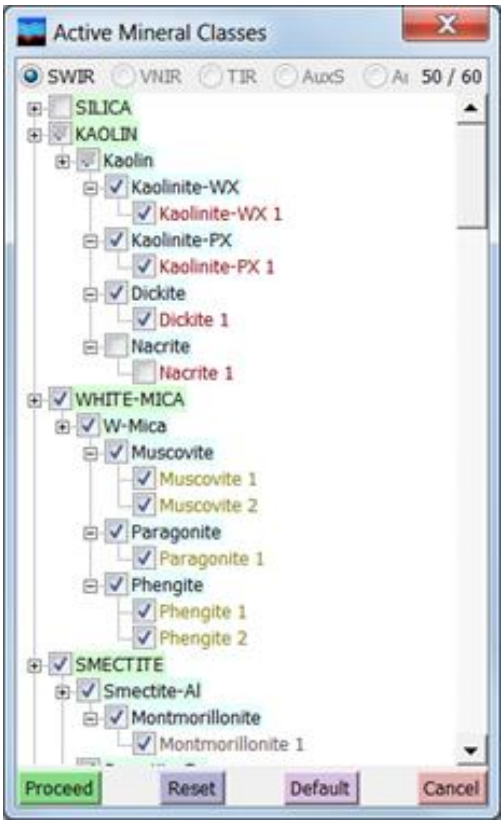

Figure 9) Example of an Active Minerals List (AML) for a dataset with some minerals turned off (improbable minerals for this specific geological setting).

TSG also provides tools for within drill hole Domaining where a further level of mineral filtering can be applied via a "Restricted Mineral Set" (RMS) that can be used to assign minerals to selected spectro-mineralogical intervals, or perhaps, lithologies or alteration zones.

5.3 Processing in TSG (SWIR)

5.3.1 Importing Spectra

Start by importing your spectra. From the “File” menu select “New”. In the dialog box that appears choose the appropriate file format. In this walkthrough we are using .asd files acquired with a Terraspec Explorer™.

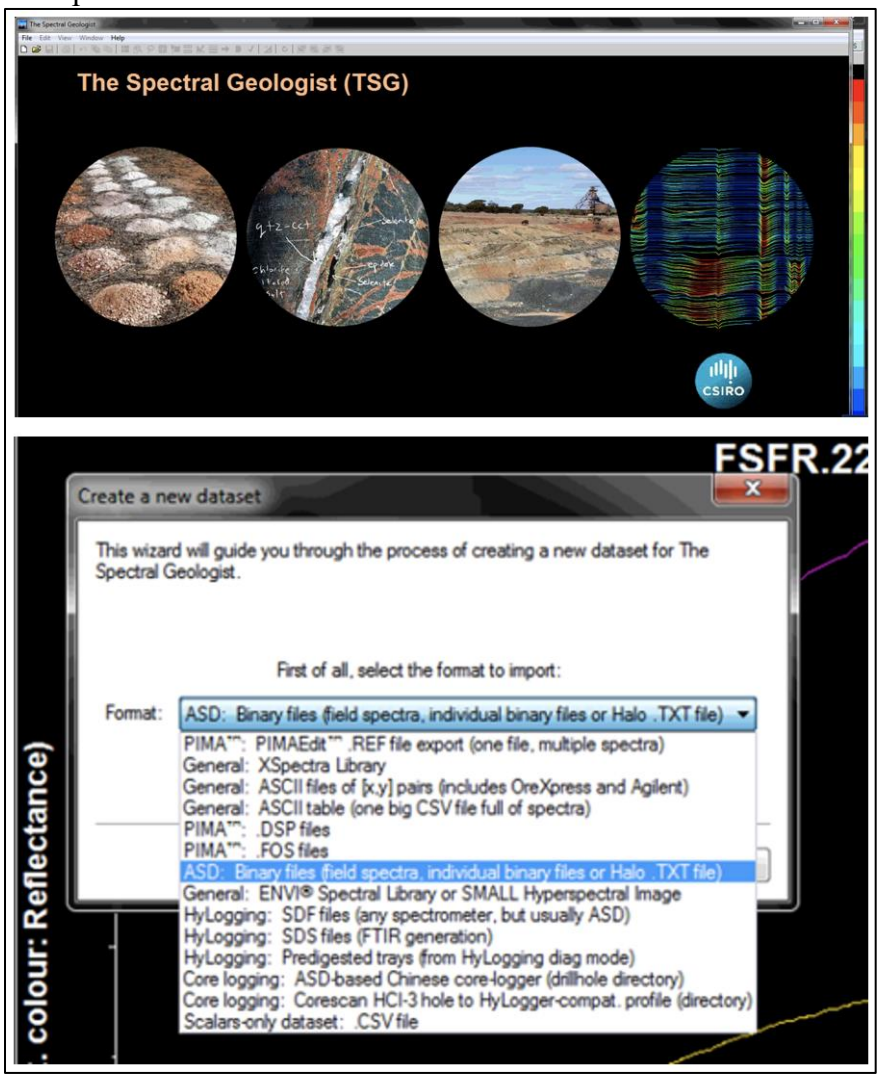

Figure 10) TSG opening screen (top), and list of importable file formats available from "File->New” (bottom).

Next, in the “Select binary ASD files (field spectra)” dialog box, browse to your spectra and select them or select a directory containing your spectra (holding down the shift button also works to select multiple spectral files). Use the settings shown in Figure 11. Note that the “Parse filenames” option may be useful if metadata like drillhole ID or meterage is embedded in the filenames of your spectra. Click “Next”.

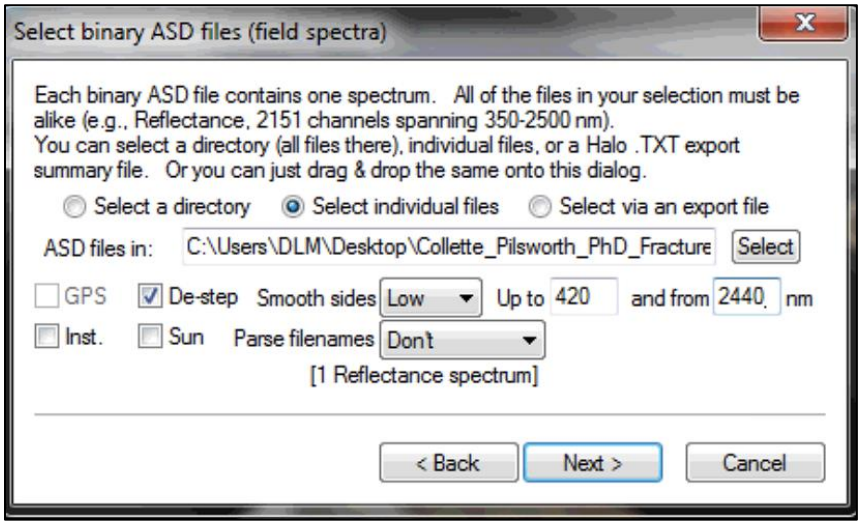

Figure 11) Setting for the import of .asd files.

In the "Wavelength info and resampling" dialog box, set the "Output wvl. Min" value to 1300 (nm) and the Max value to 2500 (nm), as shown in Figure 12. This restricts the smoothing operations and region to be interpreted by TSA to SWIR. Click "Next".

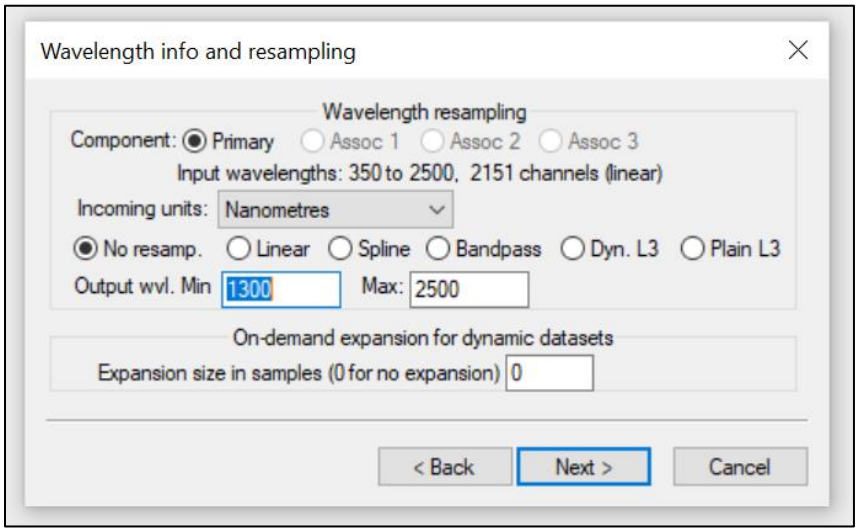

Figure 12) Further settings for the import of spectral files. Note that the output wavelength minimum has been set to 1300 nm (bypassing the VNIR range).

In the "Additional info" dialog box, shown in Figure 13, select "Spectralon absolute reflectance (generic)" as the final correction spectrum, provided that the white reference used during capture was indeed Spectralon™ (generally the case). Click "Finish". At this point the software will import your spectra, prepare them according to the previously described settings, and TSA will produce mineral matches.

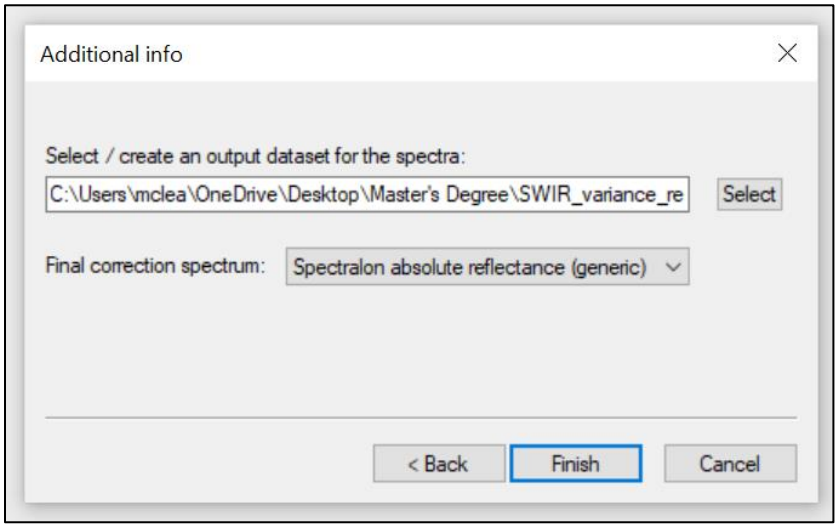

Figure 13) Final step of the import process. Definition of a save location for the .tsg file to be generated and setting the correction spectrum to Spectralon.

Notice that even very large datasets are processed almost instantly. This is the benefit provided by TSG in comparison to manual interpretation. An experienced interpreter might be able to identify more minerals but would take exponentially longer to do so and may struggle to maintain consistency. For large, systematically collected datasets, the speed and consistency benefits of TSG far outweigh the costs.

5.3.2 Navigating TSG

In the top right-hand corner of the software, you'll find buttons labelled "Summary", "Log", "Spectrum", "Stack", and "Scatter". These will direct you to views into distinct functions. The "Summary" view (Figure 14) shows summary scatterplots for a broad overview of the classified dataset.

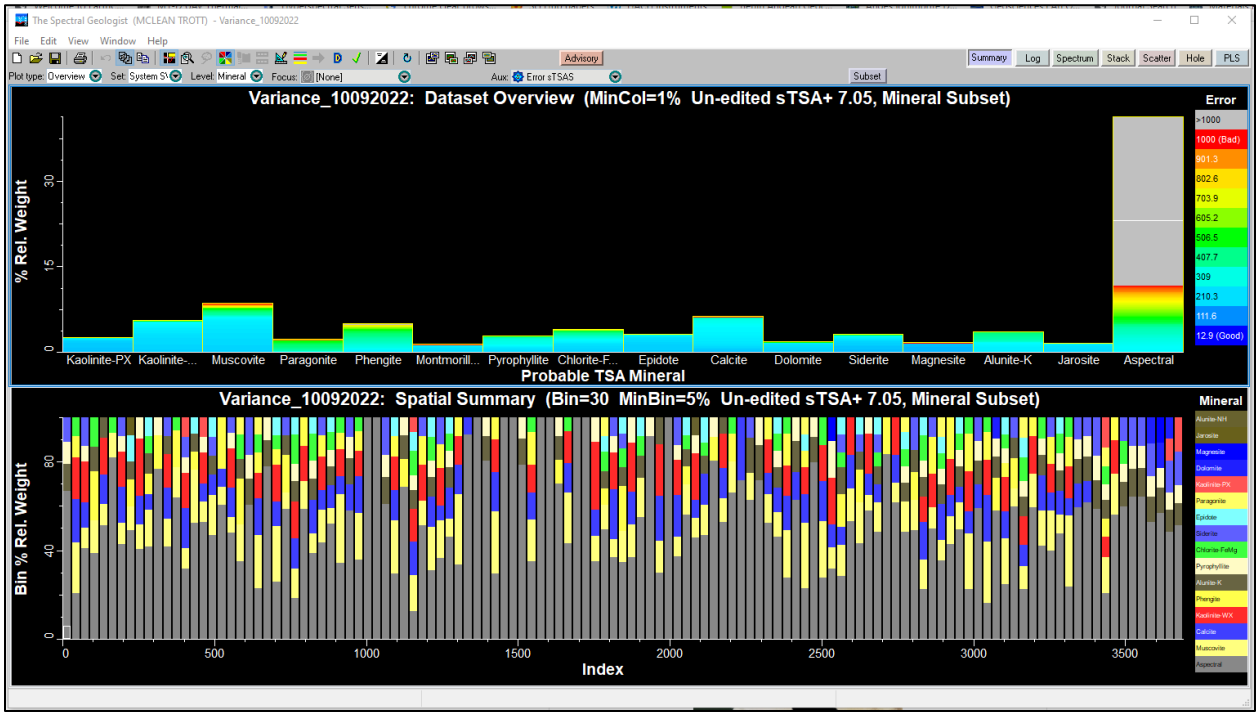

Figure 14) Summary view of the imported dataset. The first view to appear after successfully importing new data.

The default “Log” view (Figure 15) will show the sample number, colored versions of the normalized spectra, up to three minerals identified by TSA (columns prefixed with Min1, Min2, Min3), and an error bar, representing how well the spectra matches to the identified minerals.

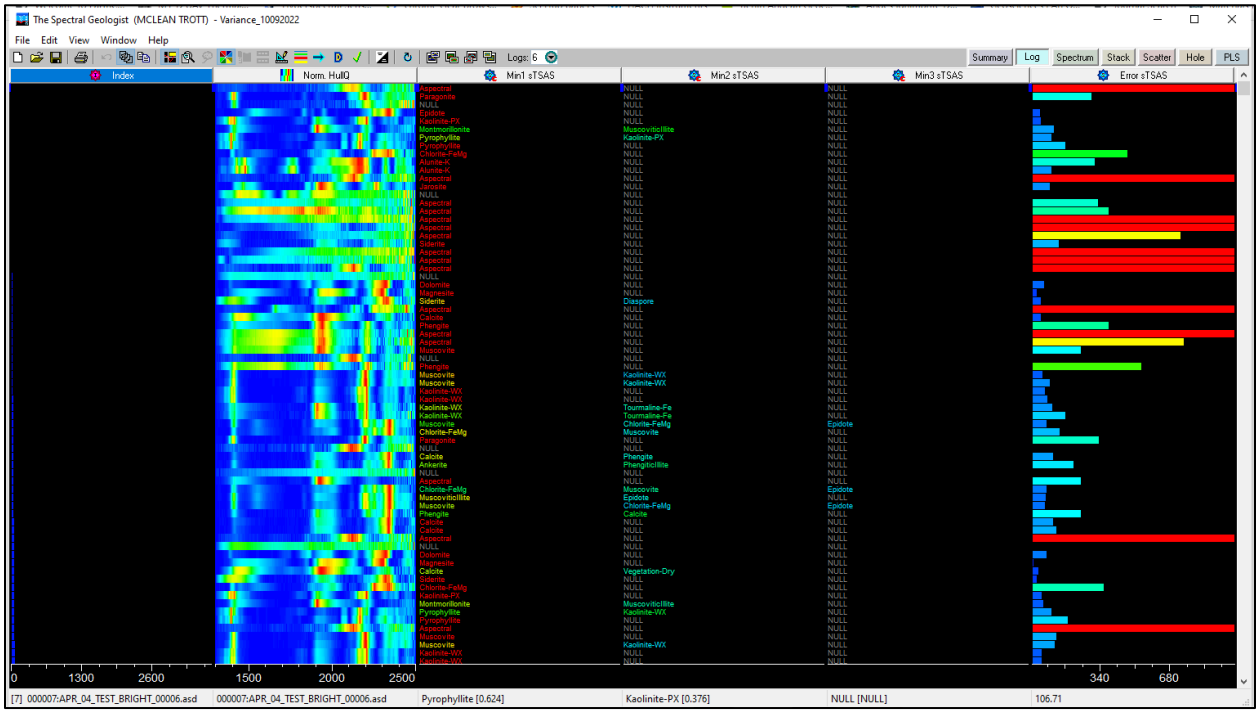

Figure 15) The 'Log' view, showing TSA mineral matches and a measure of error, alongside a top-down representation of the spectra.

The “Log” view can give a first impression about the quality of the dataset. The column labelled “Norm. HullQ” contains a colored, top-down view version of the Hull normalized (smoothed) spectrum for each sample, where blue indicates high reflectance and red indicates absorption, as illustrated in Figure 16.

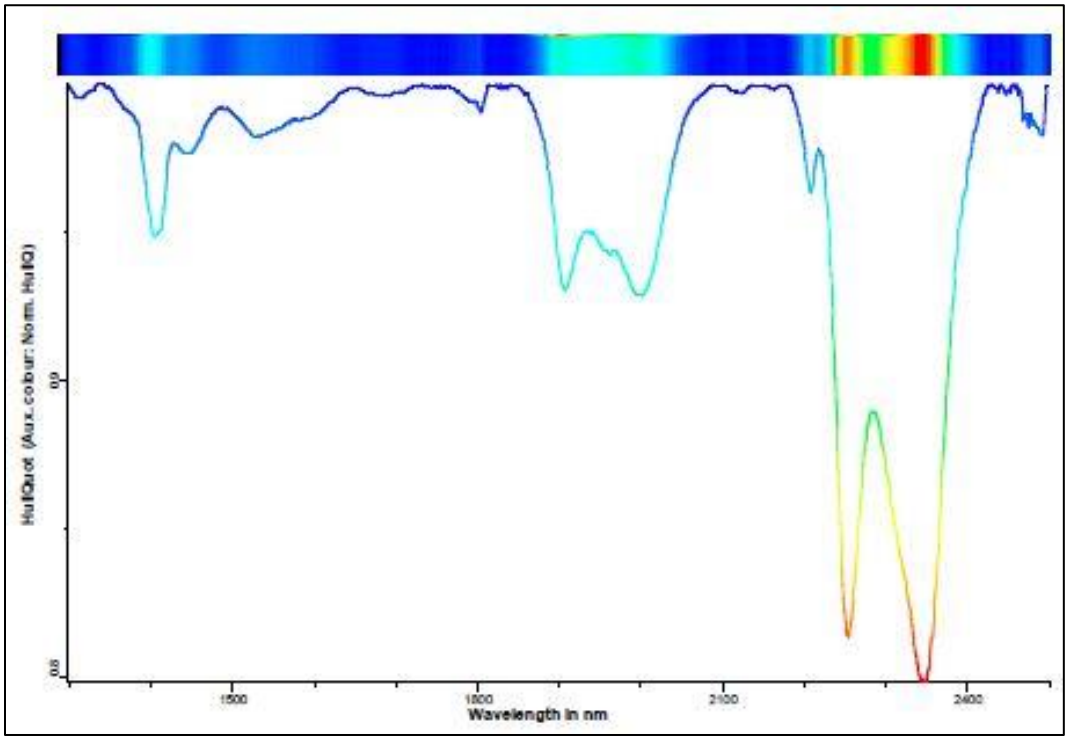

Figure 16) Illustration of how a spectra is represented as a colored band in the software, where the depth of absorptions corresponds to hotter colors.

Figure 17 shows good quality spectra (left), with little noise, where absorption features are crisp and clearly defined. Spectral quality is much poorer in many cases on the right, where the bars look noisy and/or striped. This may be due to a lack of white referencing, leading to sensors drifting over time and creating offsets in the intensity results.
Other sources of poor-quality spectra may include:

- Wet or dirty samples at the time of acquisition,
- Poor contact between the probe and the sample, permitting entrance of ambient light,
- Loose or partially broken fiber optic cable between the probe and processing unit.

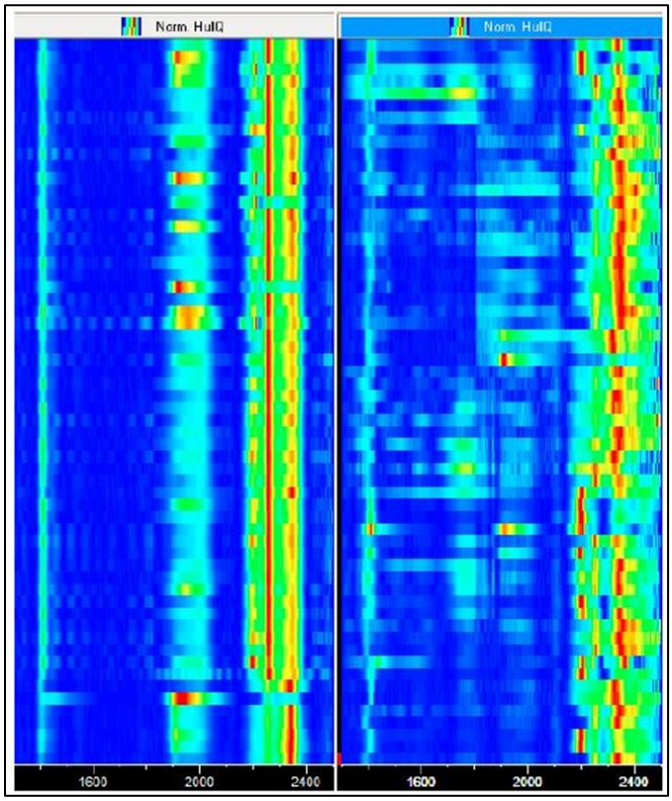

- **Figure 17) Comparison of some generally good data (left) and some poorer quality data (right).**

It is important to realize that not every mineral is active in the SWIR range. This is particularly true for minerals without bound water, ammonium, or OH- bonds. In other words, anhydrous minerals are unlikely to be detectable.
For instance, spectra may come back "aspectral" if taken on rocks with:

- Abundant plagioclase
- Massive SiO2
- Dark colours and low reflectance as a result.

In other words, "Aspectral" readings do not necessarily indicate poor quality spectra; they may be telling you something about the mineralogy of that sample (more specifically, that OH- bonds aren't present in the minerals under the probe, Figure 18). This might be important information in a scenario where one of the alteration facies consists of widespread, pervasive silicification, for example.

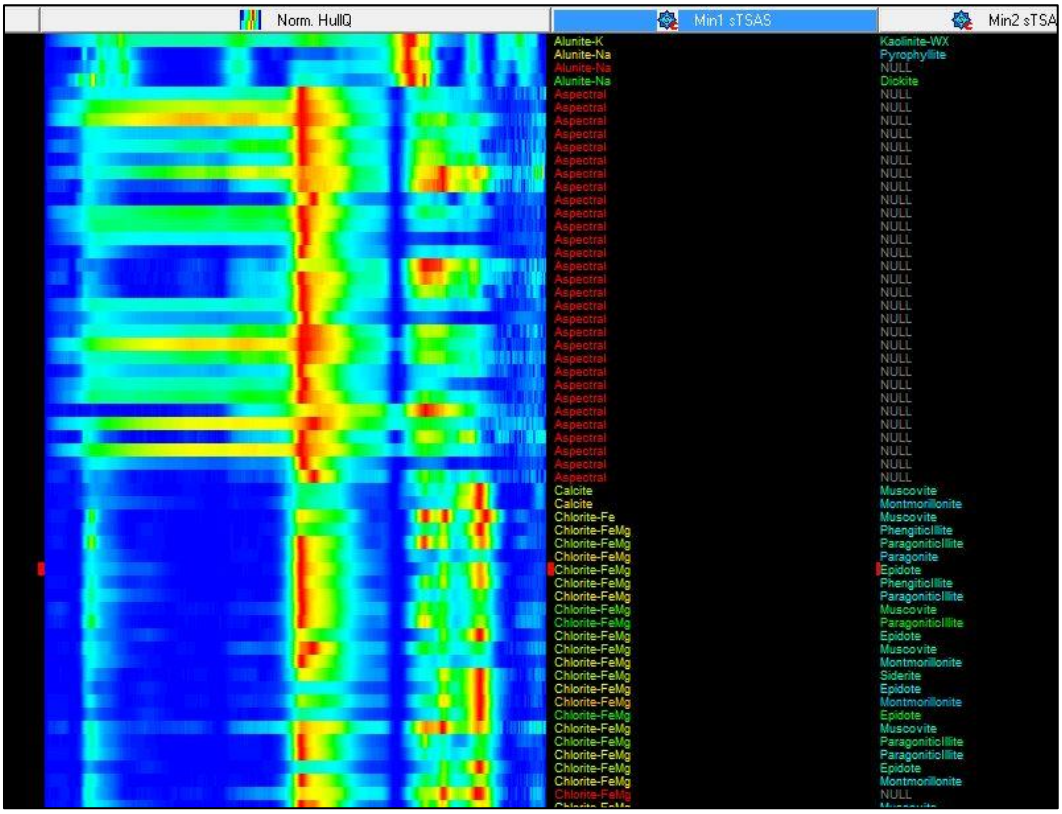

Figure 18) "Aspectral" readings in the above dataset are not all poor quality data. Some of these represent samples taken over areas of the rock that do not contain SWIR-active minerals.

In the "Spectrum" view, spectra from your dataset may be visually compared to spectra from the inbuilt TSG library. This may prove useful in cases where TSA results are ambiguous. With the "SWIR TSA" radio button activated (Figure 19) two lists will appear on the lefthand side of the view, where a spectrum from the imported data may be selected ("Sample") in addition to a reference spectrum ("Reflib").

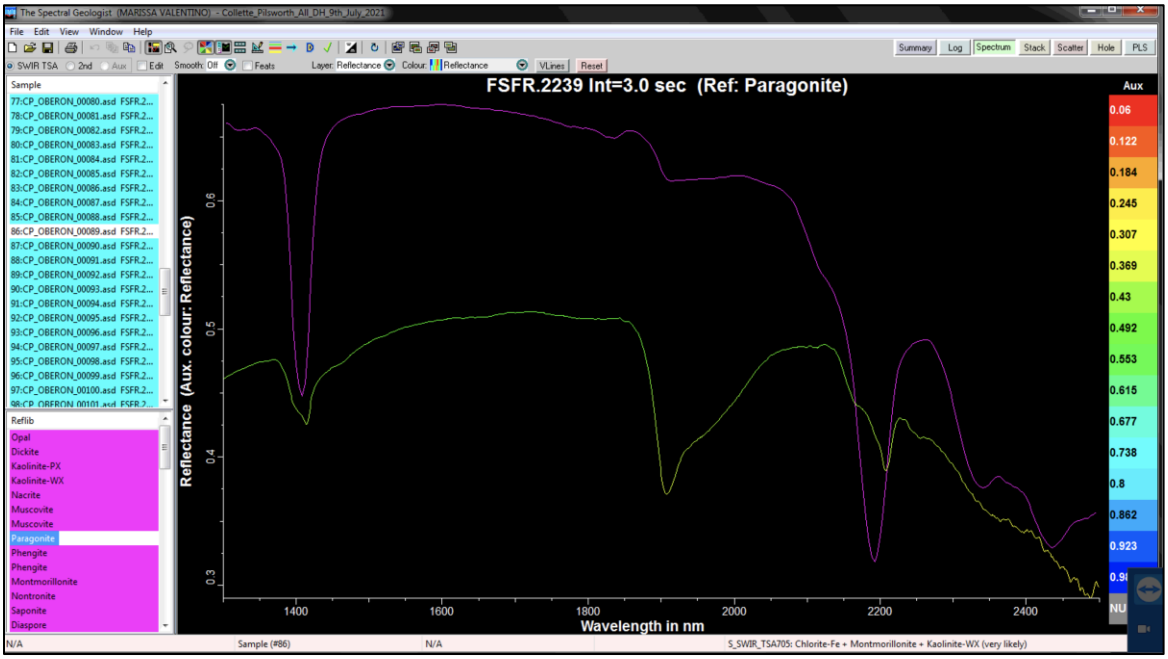

Figure 19) "Spectrum" view with the "SWIR TSA" radio button selected. A measured spectrum (green to yellow trace) is being compared to a reference spectrum for paragonite (pink trace) in this example.

Activating the "2nd" radio button will allow comparison between two collected spectra, as shown in Figure 20.

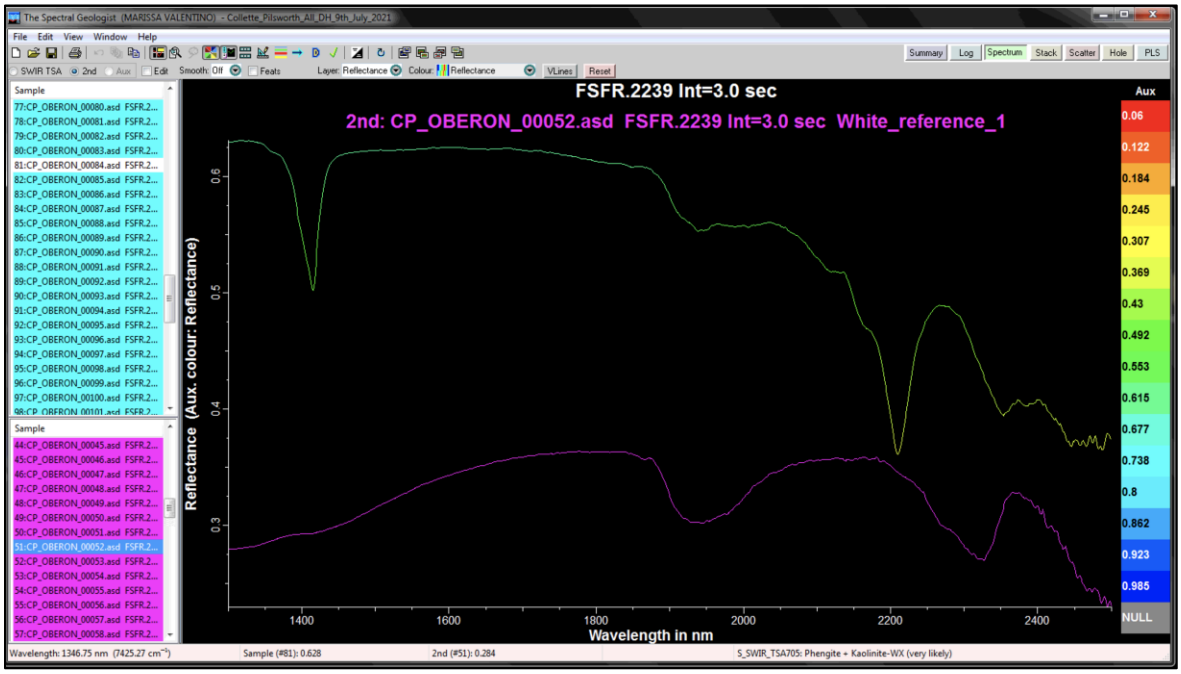

Figure 20) "Spectrum" view with the "2nd" radio button selected. Two measured spectra are being compared in this example.

5.3.3 Extracting Scalars using a Template

TSG enables application of scalars using a template, where the scalar methods used in an existing .tsg file can be applied to a recently imported dataset. This is a time-saver and ensures that calculations are being carried out consistently between datasets.
From the “File” menu hover over the “Copy processing” menu and select “Scalars and layout” from the submenu that appears. Select the template (existing .tsg file) from which you’d like to copy the scalars and order and they will be applied to the newly loaded dataset. The provided template, “SWIR_scalars.tsg” contains a variety of useful scalars, described in Table 3. Note that a .tsg file needs to be accompanied by the corresponding .bip and .ini files.

Scalar	Type	Description
Min1 sTSAS	System SWIR (TSA)	Most prominent mineral match.
Wt1 sTSAS	System SWIR (TSA)	Spectral weight of Min1. The sum of Wt1, Wt2, and Wt3 is always 1.
Min2 sTSAS	System SWIR (TSA)	2nd most prominent mineral match.
Wt2 sTSAS	System SWIR (TSA)	Spectral weight of Min2. The sum of Wt1, Wt2, and Wt3 is always 1.
Min3 sTSAS	System SWIR (TSA)	3rd most prominent mineral match.
Wt3 sTSAS	System SWIR (TSA)	Spectral weight of Min3. The sum of Wt1, Wt2, and Wt3 is always 1.
Error sTSAS	System SWIR (TSA)	A measure of the error associated with mineral matches.
SNR sTSAS	System SWIR (TSA)	Signal-to-noise ratio.
Bound_Water sTSAS	System SWIR (TSA)	"Spectral abundance" of bound water.
Unbound_Water sTSAS	System SWIR (TSA)	"Spectral abundance" of unbound water.
1400W	PROFILE	Wavelength position at minimum of 1400 nm water absorption.
1400D	PROFILE	Depth of 1400 nm water absorption.
1400FWHM	PROFILE	Width halfway up the 1400 nm water absorption feature.
1480W	PROFILE	Wavelength position at minimum of alunite absorption feature. Proxy for Na:K in alunite.
1480D	PROFILE	Depth of 1480 nm absorption feature for alunite ("spectral abundance").
1900D	PROFILE	Depth of 1900 nm water absorption feature ("spectral abundance").
2200W	PROFILE	Wavelength position at minimum of 2200 nm ("AlOH") absorption feature.
2200D	PROFILE	Depth of the 2200 nm ("AlOH") absorption feature.
2200FWHM	PROFILE	Width halfway up the 2200 nm ("AlOH) absorption feature.
2250W	PROFILE	Wavelength position at minimum of 2250 nm ("FeOH") absorption feature.
2250D	PROFILE	Depth of the 2250 nm ("FeOH") absorption feature.
2250FWHM	PROFILE	Width halfway up the 2250 nm ("FeOH) absorption feature.
2340W	PROFILE	Wavelength position at minimum of 2340 nm ("MgOH") absorption feature.
2340D	PROFILE	Depth of the 2340 nm ("MgOH") absorption feature.
2340FWHM	PROFILE	Width halfway up the 2340 nm ("MgOH) absorption feature.
amph_talc_abundance	ARITHMETIC	Spectral abundance of amphibole and/or talc minerals.
clays_kaolin_abundance	ARITHMETIC	Spectral abundance of kandites.
ill_ser_crystallinity	ARITHMETIC	(Relative) crystallinity of white micas.
kaolin_crystallinity	ARITHMETIC	(Relative) crystallinity of kandites.

Table 3) Brief descriptions of the scalars displayed in the SWIR_scalars.tsg template.

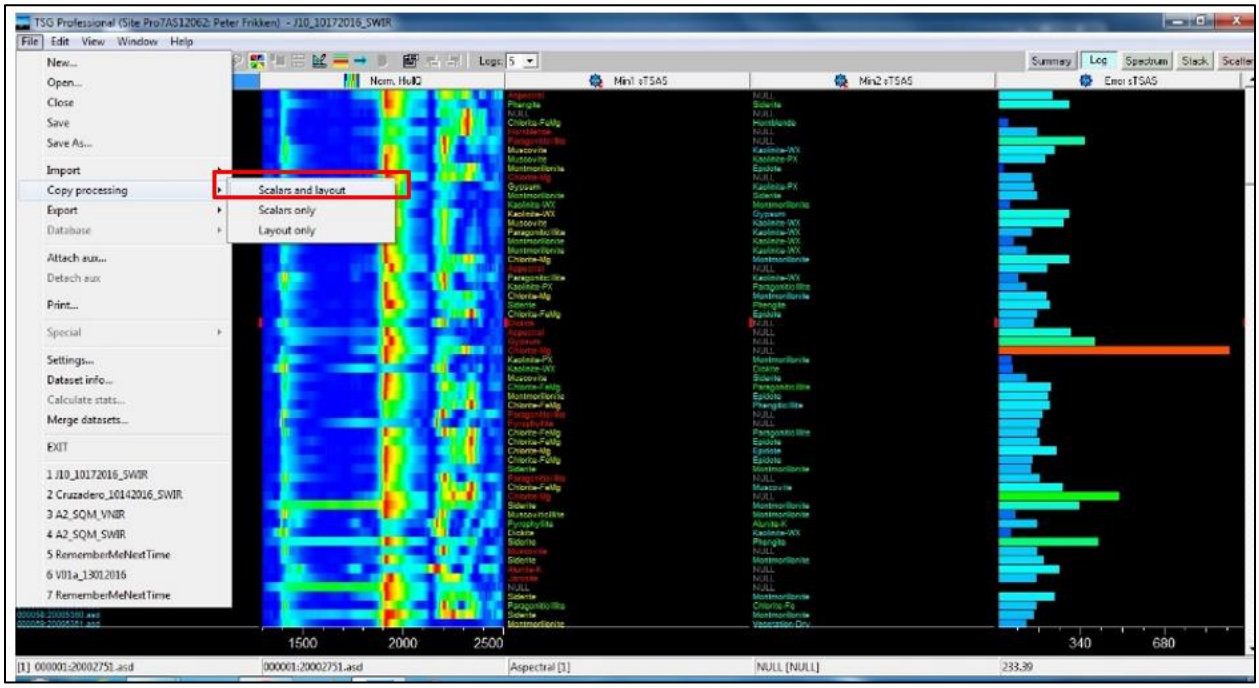

Figure 21) Perhaps the most useful functionality of TSG, scalar calculations and layout can be replicated from an existing .tsg file, by selecting the file via "File->Copy Processing->Scalars and layout".

5.3.4 Creating and Adding Custom Scalars

If you'd like to create a new scalar, click "new scalar" from the "Edit" menu.
The "Construct/Import Scalar" window will appear. We will examine the construction of a simple "PROFILE" scalar. Select this from the "Method" dropdown menu and hit "Next" (Figure 22).

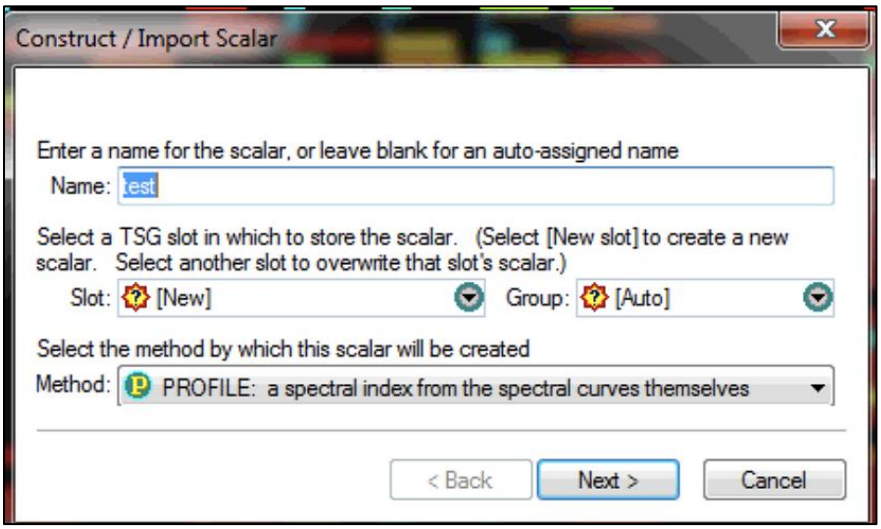

Figure 22) The first step in creating a custom scalar. "Slot" and "Group" pertain to where the scalar will be stored. "Method" indicates the type of scalar to be created, in this example "PROFILE" refers to a measurement of geometry taken directly from the spectra.

The settings shown in Figure 23 will produce a W2200 scalar, where the position (in nm) of the wavelength minimum found 10 nm to either side of 2200 nm will be the output.

Choosing “Relative absorption width” will produce the D2200 scalar (absorption depth), or “Absorption or peak FWHM” will produce the FWHM2200 scalar.
Other “Method” settings enable different styles of scalars. For instance, an “ARITHMETIC” scalar is a calculation performed on other scalars, like division of D2200 by D1900 to produce a white mica crystallinity output.

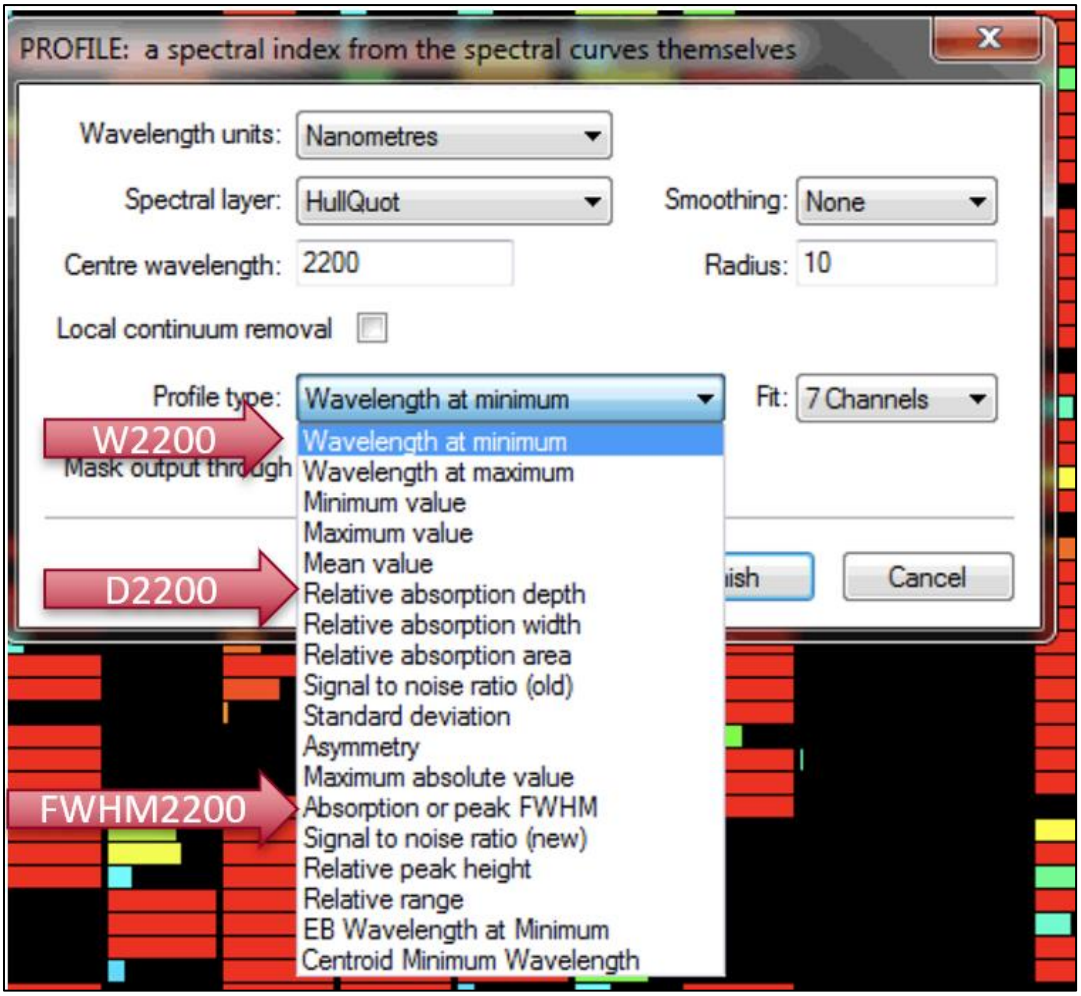

Figure 23) Example of the setup for a W2200 scalar, and how the same setup could be modified for D2200 or FWHM2200. With these settings geometry is measured from a region of the spectra centred at 2200 nm and extending 10 nm to either side (2190 – 2210 nm range).

Newly created scalars can be added to the “Log” view as desired. To visualize a scalar, right click any scalar, and select “Insert column” from the “Edit / Add / Del” submenu. If 32 scalars are already present in the view it will be grayed out and you will need to replace a scalar that is currently visualized (Figure 24).

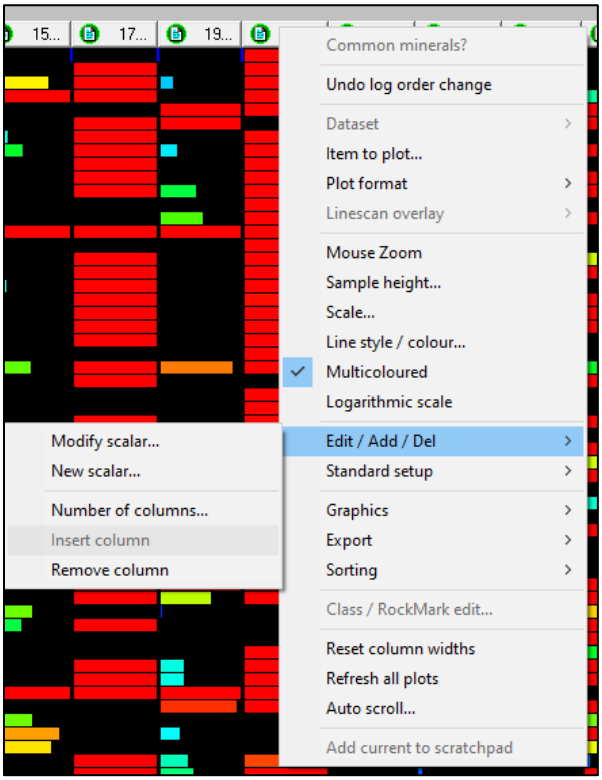

Figure 24) Menu path to insert a new scalar column. In this example 32 scalars are already displayed so the option is grayed out. In this case a scalar would need to be deleted to enable this option or an existing scalar plot modified using the "Item to plot" option.

If you successfully inserted a new column, a copy of the last scalar will appear at the far right-hand side of the "Log" view. Right click this new column (or another column that you would like to replace) and click "Item to plot…" (Figure 25).

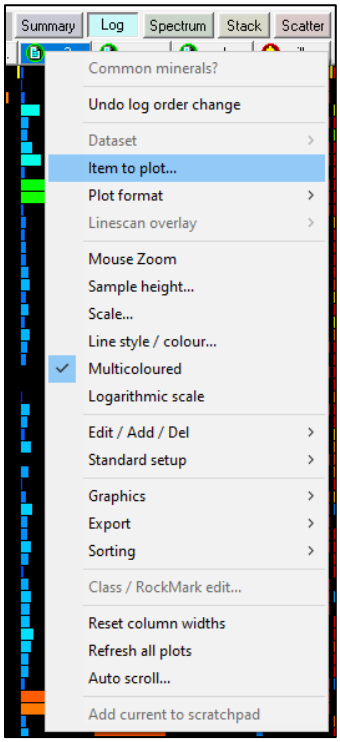

Figure 25) "Item to plot..." allows the user to select which scalar to visualize in the selected column.

In the subsequent menu, "Item for Log Column" (Figure 26), you'll be able to select from inbuilt TSA scalars ("System SWIR") or choose a custom scalar ("General"). The selected column will be replaced with the chosen scalar.

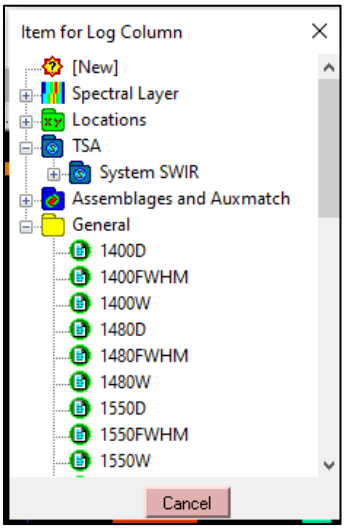

Figure 26) Preconfigured scalars may be found in 'TSA->System SWIR' or custom scalars might be stored under 'General'.

Saving the active .tsg file after adding new scalars means that they will be automatically calculated for future datasets when the current .tsg file is applied as a template through "Copy processing" as described above.

At this point the “Log” view should be crowded with scalars copied from the template and any new scalars you may have added (Figure 27). The current version of TSG allows 32 scalars to be visualized on the Log page.

Figure 27) A full set of scalars visualized. This screen is difficult to parse visually but does indicate which columns will be included in the subsequent csv export.

5.3.5 Exporting from TSG

At this point it is advisable to export the raw spectra as a table of spectra (rows) vs reflectance per band (columns). Storage of raw data is an important and often overlooked step prior to spectral processing. Individual spectral files (e.g., *.asd, *.sed, *.ascii) can be saved along with their corresponding metadata. However, the most ideal format is as tabular spectra that can imported into a relational database linked with the spectral interpretation and any other geoscientific data (e.g., geochemistry). Preserving raw spectra permits consistent interpretation when new data is added to a project or future reprocessing using new advancements.
An interesting quirk of TSG is that export options in the File menu are dependent on the current view. To export raw data in a tabular format, navigate to the “Stack” view, and then select “Export to CSV (spectra)” from the File menu (Figure 28). This will export a .csv file of the dataset where reflectance is assigned to bands (columns) for each sample (row). This is a format that lends itself to import into a relational database, and where the sample ID can be used to link the spectra to its metadata or additional accompanying data.

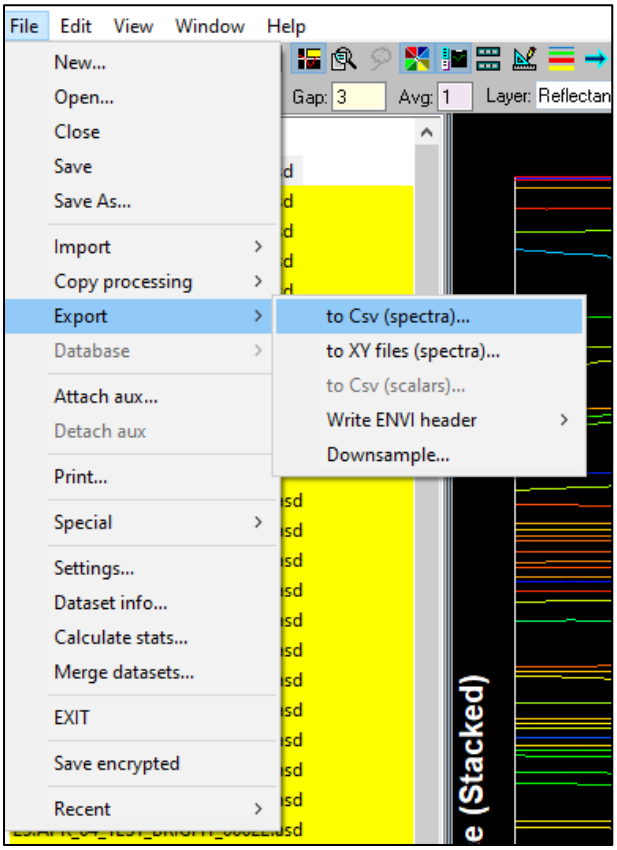

Figure 28) Export of raw spectral data in tabular format must be done from the "Stack" view, following "File->Export->to Csv (spectra)...".

Save the exported spectra into a relational database, along with the metadata captured with it. When you add new data from your project, or add a new and exciting scalar, you can import it back into TSG and process it again, by choosing the "General: ASCII table (one big CSV file full of spectra)" format in the "Create a new dataset" dialog box.
Once the raw data is exported and saved for future use, switch the view over to "Log". You'll notice that in the File->Export submenu "to Csv (spectra)" is now grayed out but "to Csv (scalars) is now available (Figure 29). Click this to export your scalar output as a .csv file.

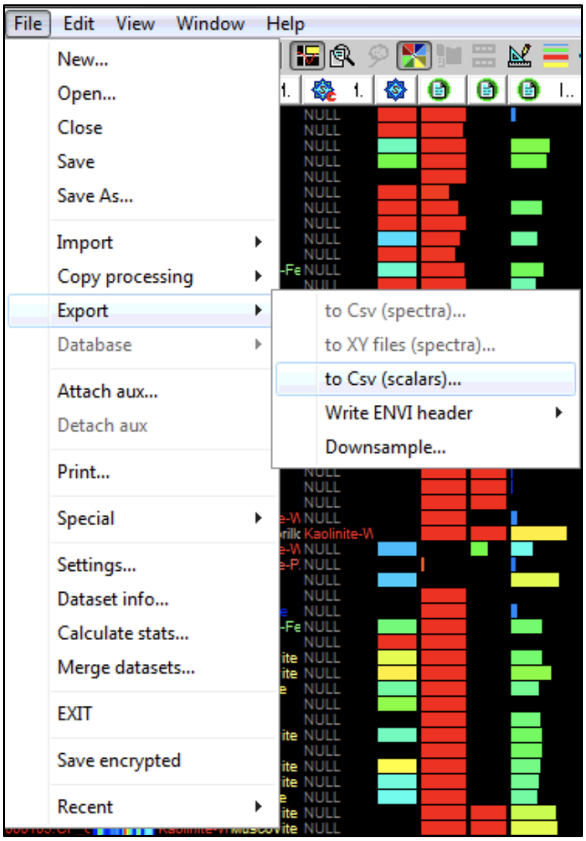

Figure 29) Notice that "to Csv (spectra)..." is grayed out from the "Log" view. Scalars can now be exported, following "File->Export->to Csv (scalars)...".

5.3.6 Cleanup of Scalar Table

Open the newly exported .csv file (the scalars). You'll see a row per sample/measurement and numerous columns corresponding to mineral matches, error, and extracted scalars. You will likely see some cells with "NULL" rather than a number; in most cases these are scalars where a given sample did not contain that absorption feature. The Error column may also have some null values, where the error calculation failed. The error is on a scale from 0 to 1000, where 0 represents a perfect spectral match to the reference library (rare), and higher values represent increasingly dubious matches. For subsequent steps you'll need a purely numeric column to plot mineral matches against. For this reason, highlight the Error column and use Excel's "Find and Replace" function to replace "NULL" with "1000".
Once this is finished, highlight the entire sheet and replace all other nulls with an empty cell (Figure 30).

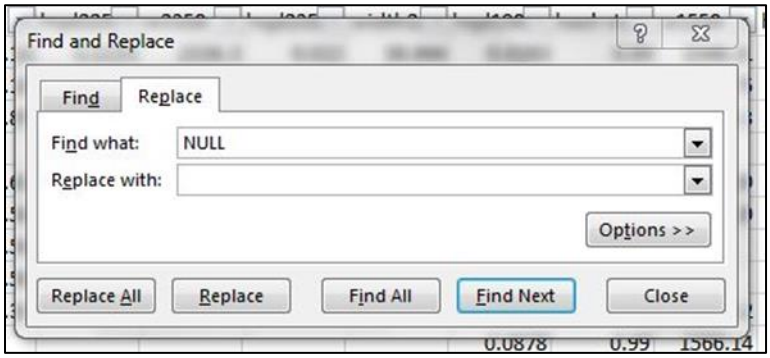

Figure 30) MS Excel's "Find and Replace" function ("Home" tab) may be used to replace NULLs in the error column with 1000 and remove all other nulls by leaving "Replace with:" empty.

Save and close the .csv file; it is now formatted such that it can be easily read by ioGAS or similar software.

The following steps are described using ioGAS software. The procedure itself can likely be carried out in a variety of software; for convenience we illustrate with ioGAS, as it contains several functions/tools which make the process straightforward. Most useful are the "point density opacity" function and "attribute polygon" tool, found on the vertical toolbar on the right-hand side of the ioGAS interface.

5.3.7 Import to ioGAS

After opening ioGAS, select "New" from the "File" menu. Set "Files of type" to "All Files" or "csv" and browse to the scalar table exported in the previous step (Figure 31). Open it.

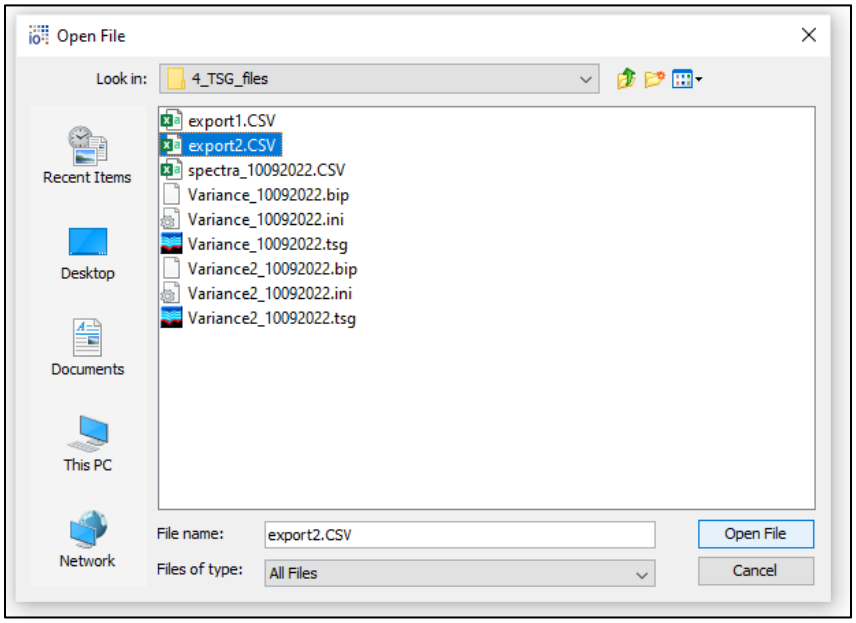

Figure 31) Importing a .csv file into ioGAS.

If an error about unequal row lengths (Figure 32) appears there is a problem in the way delimiters are being parsed. In this situation, cancel the import, save a version of the .csv file as a .xlsx, and open it into ioGAS in that format.

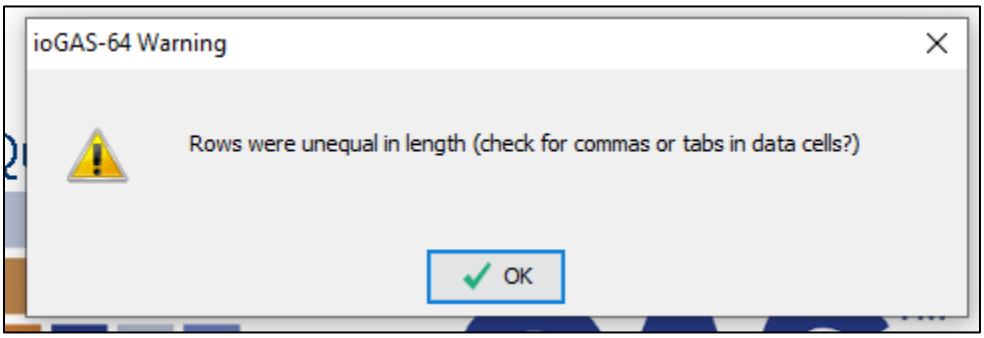

Figure 32) If this warning appears while importing a .csv file, convert the file to .xlsx format and import it again.

When the "Column Properties" dialog appears, look at the "Alias" and "Type" columns (Figure 33). Most of the columns should be of type "Numeric" (blue circles). The mineral match (Min1, Min2, Min3) columns should be of type "Text" (black circles). If the NULLs were improperly removed in the previous step, some columns for scalar values which should be numeric may attempt to default to text. If this is the case open the .csv and find/replace NULLs carefully, as described previously. SpectralID and Date will most likely default to "Text" type, which is fine.

- At no point during this process should you ever click the "Guess Aliases" button. This is an ioGAS function, extremely useful for geochemical data, which will attempt to recognize geochemical data columns appropriately. In the case of SWIR scalar outputs, it will just make a mess attempting to match scalar names to elements from the periodic table.

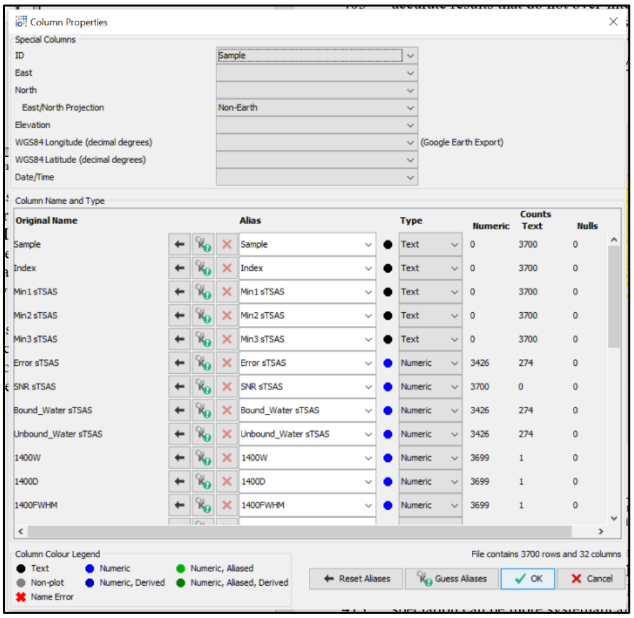

Figure 33) Provided all the NULL replacements were carried out successfully, no modifications should be needed in the "Column Properties" dialog. NEVER select "Guess Aliases".

Click 'OK' to finish importing your data into ioGAS.

5.3.8 Mineral Groupings

TSG mineral matches are algorithmically driven and anchored to a reference library; nature abhors absolutes and as a result many mineral matches may be too specific and unrealistic. Manually generalizing some results into mineral groups is the most reliable way to arrive at accurate results that do not over-interpret the mineralogy. White mica minerals are a prime example of this; TSG will match a spectra containing white mica to any of: paragonite, illitic paragonite, muscovite, illitic muscovite, illitic phengite, and phengite, as these are the white mica minerals found in its spectral library (Figure 34).

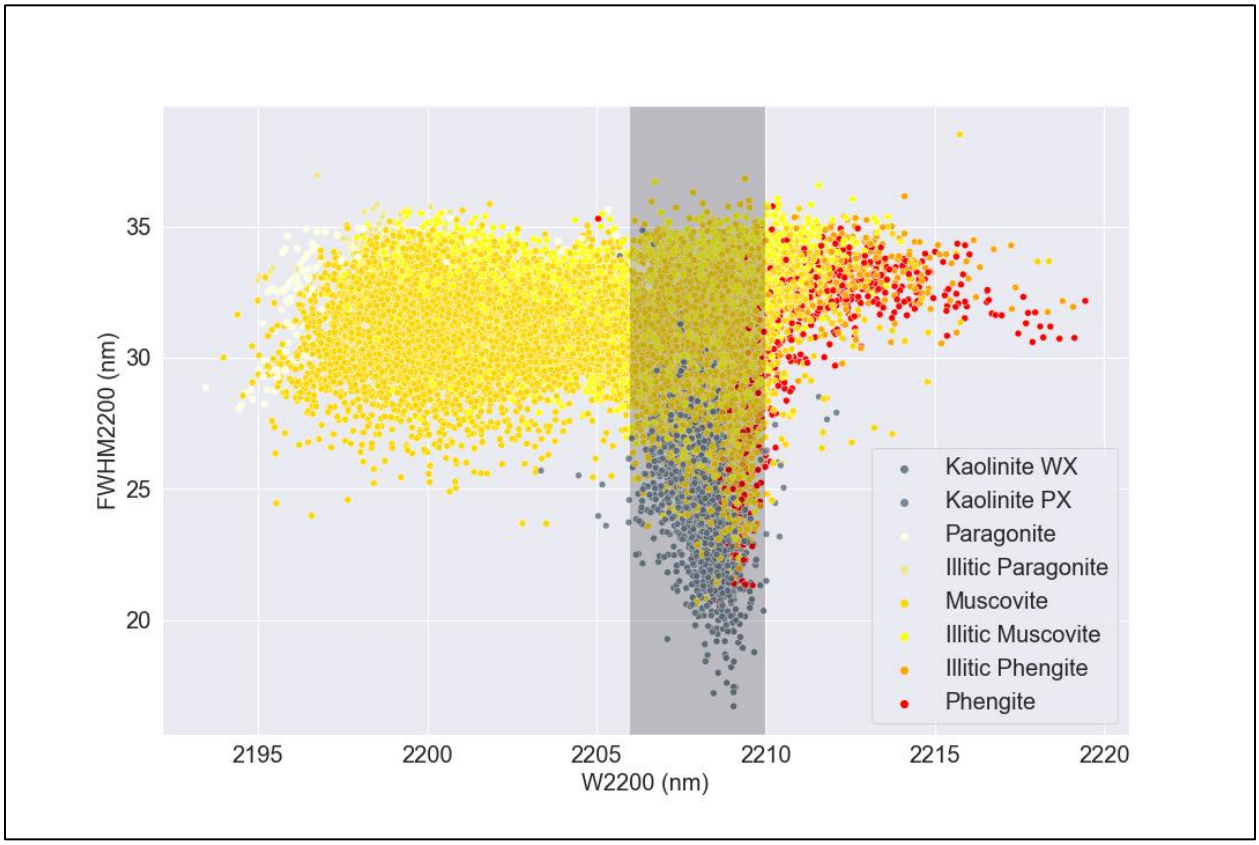

Figure 34) Some of the white mica and kaolinite variants matched by TSA. While the white mica variants are almost certainly white micas, compositional distinctions are better determined through examination of the W2200 value.

While there are undoubtedly different species of white mica in many datasets, TSG doesn't necessarily separate them robustly. For this reason, it is important to group these highly specific mineral matches into a more general "White Mica" class. In the case of white mica minerals, speciation can be more systematically evaluated using the W2200 value. The same logic applies to kaolinite (Kaolinite-WX and Kaolinite-PX may be grouped) and several other mineral classes (carbonates and amphiboles most notably). See Table 4 for suggested groupings. The grouping scheme is geared toward the porphyry/epithermal environment; distinct groupings and/or nomenclature may be useful in other environments. The white mica – kaolinite and white mica – chlorite mixtures, however, should be determined this way regardless of environment, for reasons detailed in "Dealing with Mixtures".

Grouping	TSG Min1	**OR** TSG Min2/Min3	**AND** TSG Min2/Min3	Comments
Hot_advanced_argillic	Pyrophyllite, Diaspore, Topaz	Pyrophyllite		Pyrophyllite spectrum is very diagnostic; reliably present in any of Min1, Min2, or Min3.
Medium_advanced_argillic	Dickite, Nacrite			Dickite and nacrite are polymorphs.
White_mica	Phengite, Paragonite, Muscovite, Illitic Phengite, Illitic Paragonite, Illitic Muscovite			
Kaolinite	Kaolinite-WX, Kaolinite-PX, Halloysite			Kaolinite and Halloysite are polymorphs.
Chlorite	Chlorite-Mg, Chlorite-FeMg, Chlorite-Fe			
Epidote	Epidote, Zoisite			Further refinement of epidote may be needed; MgChlorite frequently misidentified as epidote.
Smectite	Palygorskite, Nontronite, Montmorillonite, Magnesium Clays			
Alunite	Alunite-K, Alunite-Na, Alunite-NH			Note that alunite may be of hypogene or supergene origin.
Biotite	Biotite, Phlogopite	Biotite, Phlogopite		Low albedo but relatively diagnostic spectra.
Amphibole	Tremolite, Riebeckite, Hornblende, Actinolite	Tremolite, Riebeckite, Hornblende, Actinolite		Low albedo but relatively diagnostic spectra.
Gypsum	Gypsum			Anhydrite (undetectable) surficially hydrates to gypsum (detectable) rapidly after drilling.
Carbonate	Siderite, Dolomite, Calcite, Ankerite, Magnesite			Default carbonate speciation is poorly done by TSA; better to view these as carbonates.
Aspectral	Aspectral, ""			
Tourmaline	Tourmaline, Tourmaline-Fe, Rubellite			
Talc_serpentine	Talc, Serpentine			
Jarosite	Jarosite			
Contamination	Teflon, Vegetation-Dry, IsaWhite, IsaYellow, Wood, PlasticChipTray, WhiteMarker, YellowMarker			Would suggest a problem at the time of acquisition.
White_mica_kaolinite_mixture	Phengite, Paragonite, Muscovite, Illitic Phengite, Illitic Paragonite, Illitic Muscovite		Kaolinite-WX, Kaolinite-PX	Further refinement using W2200 vs FWHM2200 required.
White_mica_kaolinite_mixture	Kaolinite-WX, Kaolinite-PX		Phengite, Paragonite, Muscovite, Illitic Phengite, Illitic Paragonite, Illitic Muscovite	Further refinement using W2200 vs FWHM2200 required.
White_mica_chlorite_mixture	Phengite, Paragonite, Muscovite, Illitic Phengite, Illitic Paragonite, Illitic Muscovite		Chlorite-Mg, Chlorite-FeMg, Chlorite-Fe	
White_mica_chlorite_mixture	Chlorite-Mg, Chlorite-FeMg, Chlorite-Fe		Phengite, Paragonite, Muscovite, Illitic Phengite, Illitic Paragonite, Illitic Muscovite	

Table 4) Suggesting groupings based on TSA-suggested mineral matches.

To generate these groupings in ioGAS, open the “Select Variables” dialog, and move the Error and Min columns to the right using the white arrow (into the “Selected” list, as shown in Figure 35). Make sure that the Error column is first in the list as it will become the common axis for three XY plots. Hit “OK”.

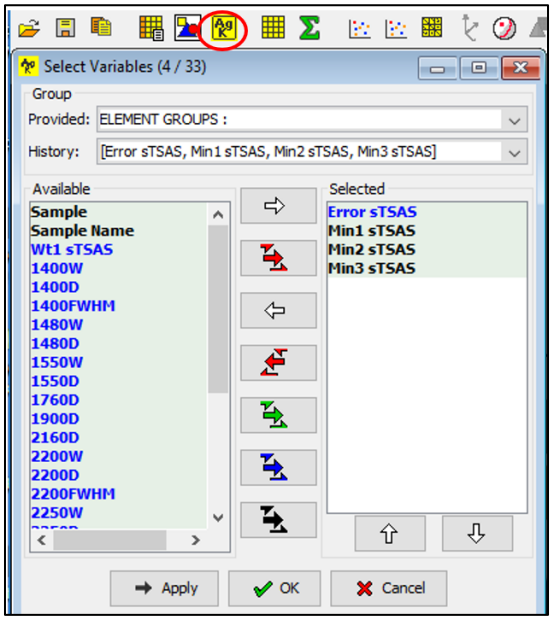

Figure 35) Selection of variables to create plots of TSA mineral matches against error.

In the upper toolbar, click the "XY Plot" icon to generate three plots of the Error against the three mineral matches. We replaced NULL with 1000 earlier; a numeric axis was required for these plots.

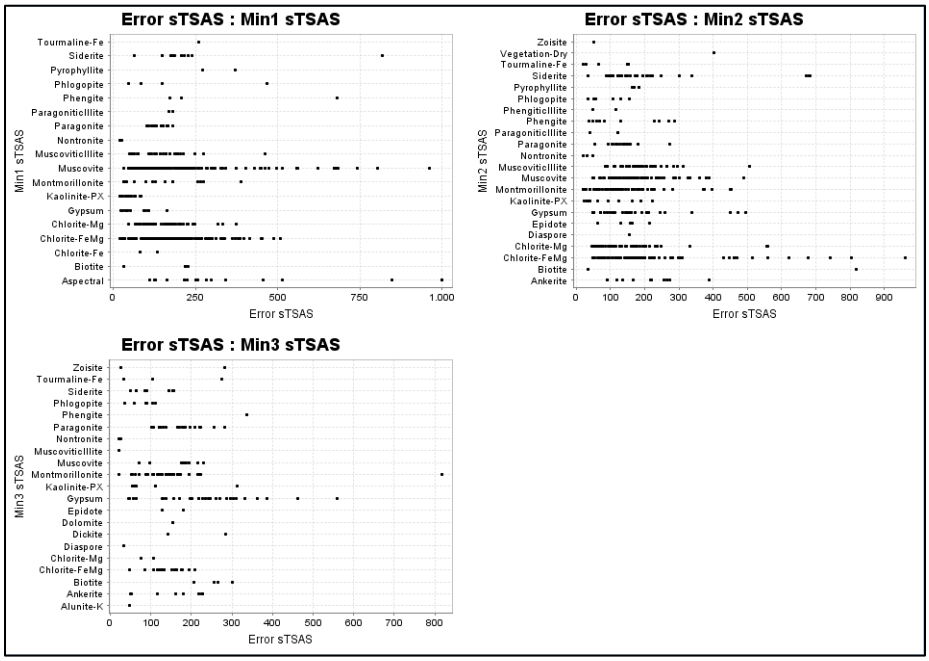

Figure 36) These plots facilitate manual regrouping of identified minerals.

At this point, open the "Attribute Manager" and set up color categories for your mineral groupings (Figure 37).

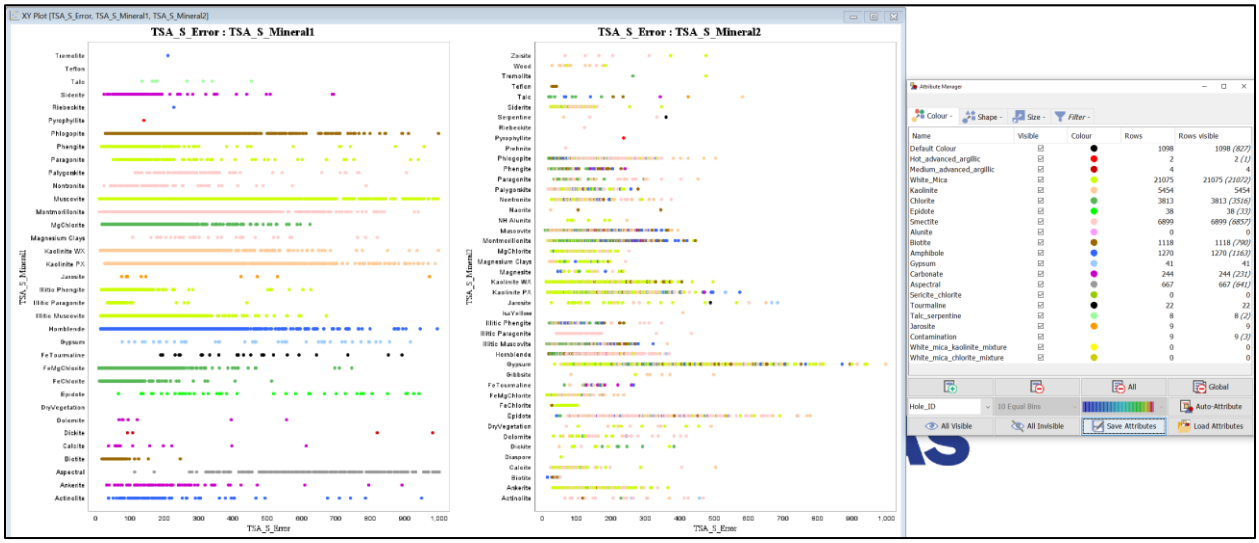

Figure 37) Example of partially regrouped mineral matches.

The .gat file accompanying this document, "Mineralogy_SWIR.gat", can be used by accessing it through the "Load Attributes" button, or you can generate your own groupings as desired. For consistency we suggest using the supplied legend in the .gat file. This will import predefined categories with assigned colors, although readings will still need to be populated appropriately, using Table 4 as reference. Highlight each mineral group in the legend one at a time, and while the correct group is highlighted, use the "Polygon Select" tool from the righthand toolbar to draw polygons around the appropriate minerals in the Min1 plot (just Min1 for now, or the strongest match per sample), thereby attributing them into the highlighted color group (Figure 37).

5.3.9 Dealing with Mixtures

Some mineral mixtures can complicate scalars used for vectoring to ore deposits.
Tschermak substitution in white micas, as quantified in the position of the 2200nm absorption feature (W2200), can be a useful vector towards hydrothermal ore deposits like porphyry copper or epithermal gold. Unfortunately, kaolinite also has an absorption at 2200nm and a much higher albedo than white mica, so in a spectrum containing both, the absorption feature will always show the position of the absorption as it relates to kaolinite, NOT the white mica. The kaolinite absorption is ALWAYS around 2207-2208 nm (it does not show systematic compositional variation like the white micas).
Meaning that this sort of vectoring is impossible in spectra containing any amount of kaolinite in addition to white mica, and hence the importance of resolving which spectra are mixtures vs pure white mica.
To resolve this better, we will create a mixed color category where samples with a white mica in Min1 and kaolinite in Min2 or Min3 can be placed; along with samples showing kaolinite in Min1 and a white mica in Min2 or Min3. Make all the color categories except "White_Mica" invisible ("All Invisible" button in the Attribute Manager). Use the "polygon select" tool to attribute the points showing "Kaolinite-WX" or "Kaolinite-PX" in the Min2 and Min3 XY plots into the "White_Mica_Kaolinite_Mixture" color category. When you've finished with that, turn everything invisible again and then make "Kaolinite" visible. Now use "polygon select" to attribute points showing any white mica species in the Min2 and Min3 plots into the mixture color category.

Repeat the above process to create mixture categories for white mica and chlorite mixtures. This combination may impact vectoring using W2250 or D2250 and should be identified for later filtering.

Returning to the white mica – kaolinite mixtures, we can further resolve this using the 2200 nm absorption feature. In the "Select Variables" dialog, move W2200 and FWHM2200 into the righthand box. Create an XY plot with W2200 on the x-axis and FWHM2200 on the y-axis. In the "Attribute Manager" make all color categories invisible except for White_mica, Kaolinite, and White_Mica_Kaolinite_Mixture. Notice the way kaolinite and mixtures group themselves in the 2207-2208 position, often at lower FWHM2200 values (Figure 38).

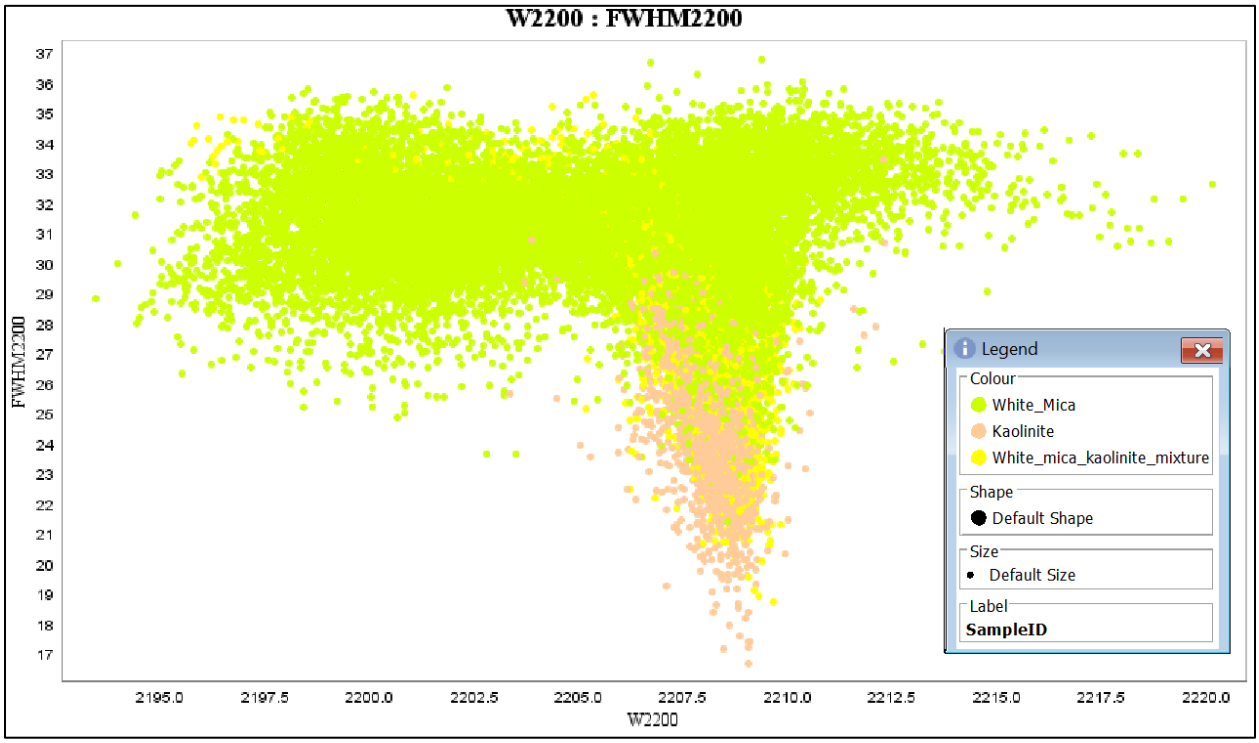

Figure 38) Samples identified in the 'White_Mica' group that are located in and around the 'Kaolinite' and 'White_mica_kaolinite_mixtures' groups in the vicinity of 2206-2209 nm may contain some influence from kaolinite and should not be used for vectoring using aspects of the 2200 nm absorption geometry.

Another useful way of visualizing these populations is by experimenting with the "Point density opacity" button on the righthand toolbar (Figure 39). Notice the left to right trend of predominantly white mica spectra and compare it to the subvertical kaolinite trend forming a triangle downward toward 2208 nm on the x-axis.

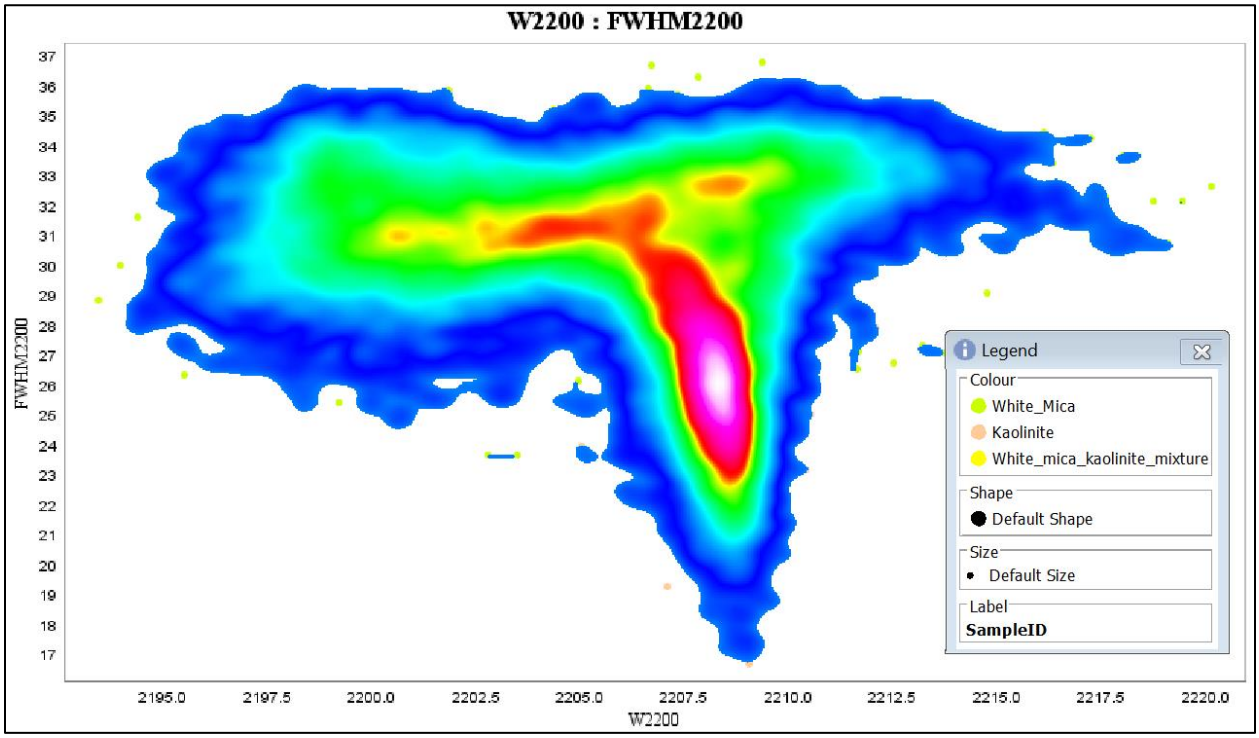

Figure 39) Point density visualization of the white mica and kaolinite subset. Note the pronounced kaolinite feature centered around 2208 nm.

Now that you've recognized where these spectra most likely contain an influence from kaolinite, make the Kaolinite category invisible and use the locations of the White_Mica_Kaolinite_Mixture spectra to re-attribute White_Mica spectra into this category with the "Polygon select" tool. Make the Kaolinite visible again. The spectra that are still in the White_Mica category can be used reliably now to vector with W2200 (white mica composition), as shown in Figure 40.

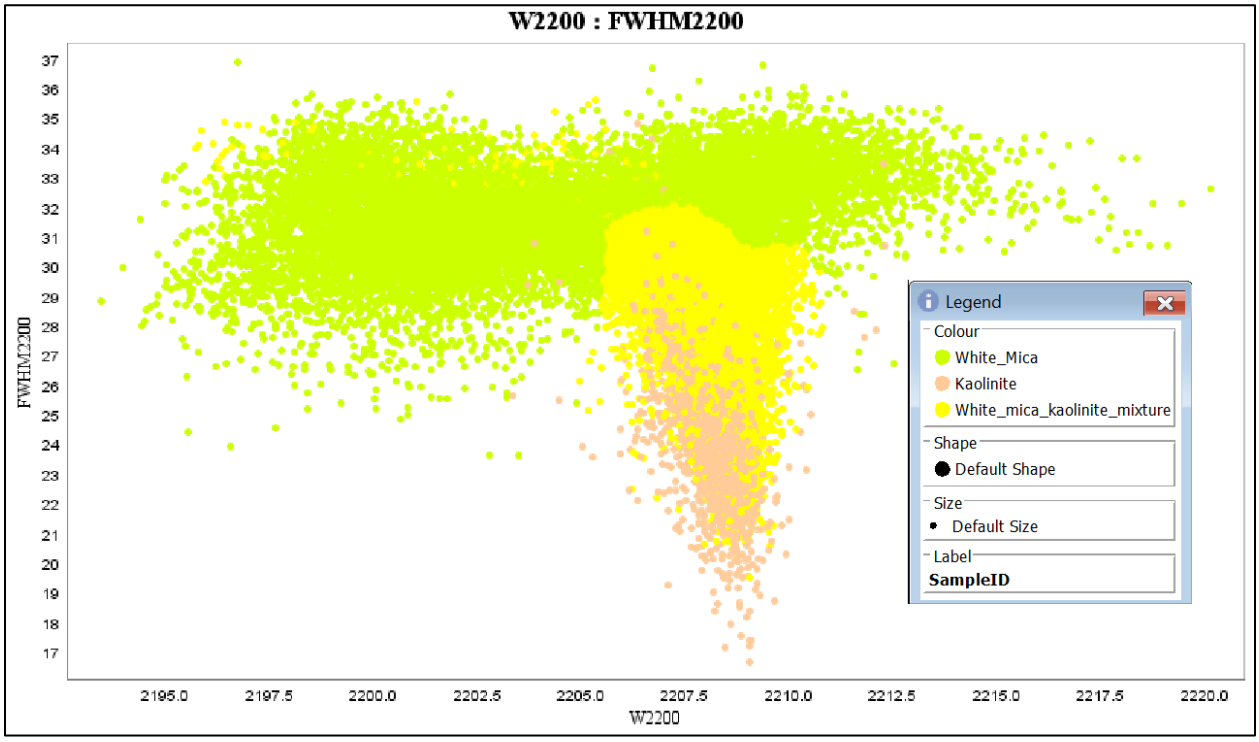

Figure 40) Illustration of how spectra with a possible influence from kaolinite might be regrouped as mixtures (and thereby disregarded for W2200 vectoring).

Once you've followed the above steps and are satisfied that you've:

- simplified any mineral species that were over-interpreted by TSG, and
- grouped and identified mineral mixtures that may impact your work,

make all the mineral groupings visible in the "Attribute Manager" and from the Data submenu of the horizontal toolbar at the top of the screen, inside the "Make Variables" section, choose "From Colour".
This will add your color groupings to the underlying data table as an additional column.
Name the new column "Mineralogy_SWIR" (Figure 41).

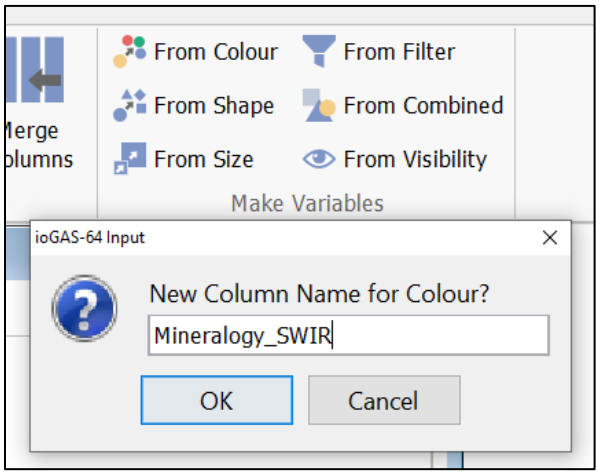

Figure 41) Saving the newly assigned groupings into the underlying data table.

5.3.10 Export and Cleanup

At this point the data table can be exported as a .csv file using the “All: export all rows” button in the “File” menu (Figure 42).

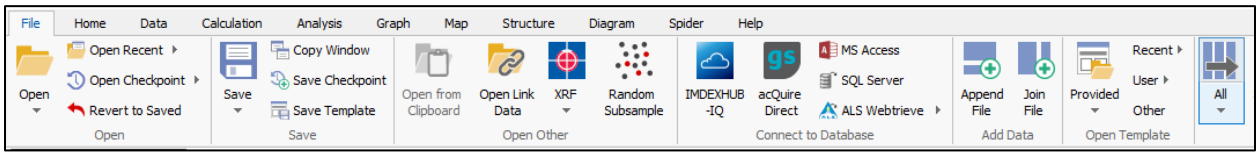

Figure 42) Export the regrouped data.

After opening the exported .csv file, you’ll notice that two columns have been added at the far right of the columns originally exported from TSG, “Mineralogy_SWIR”, containing numbers, and “Mineralogy_SWIR Text” containing the groupings created earlier (as text, shown in Figure 43). The “Mineralogy_SWIR” column can be deleted; it is simply a numeric version of the mineral groupings. After deleting this column, rename “Mineralogy_SWIR Text” to “Mineralogy_SWIR”. These groupings will be used to filter columns to valid vectors.

AI	AJ
Mineralogy_SWIR	Mineralogy_SWIR Text
19	White_mica_kaolinite_mixture
3	White_Mica
19	White_mica_kaolinite_mixture
3	White_Mica
19	White_mica_kaolinite_mixture
19	White_mica_kaolinite_mixture
19	White_mica_kaolinite_mixture
19	White_mica_kaolinite_mixture
19	White_mica_kaolinite_mixture
19	White_mica_kaolinite_mixture
19	White_mica_kaolinite_mixture
19	White_mica_kaolinite_mixture
3	White_Mica
4	Kaolinite
3	White_Mica
19	White_mica_kaolinite_mixture
19	White_mica_kaolinite_mixture
19	White_mica_kaolinite_mixture
19	White_mica_kaolinite_mixture
3	White_Mica
19	White_mica_kaolinite_mixture
19	White_mica_kaolinite_mixture

Figure 43) Two new columns added to the exported data. The numeric column can be deleted, and the word 'Text' removed from the heading of the text column.

Find the “W2200”, “D2200”, and “White_mica_crystallinity” columns. Copy/paste them at the righthand side of the “Mineralogy_SWIR” column.

Highlight all your data by clicking the top left corner of the excel sheet and then from the File menu choose “Filter” below “Sort & Filter” (Figure 44).

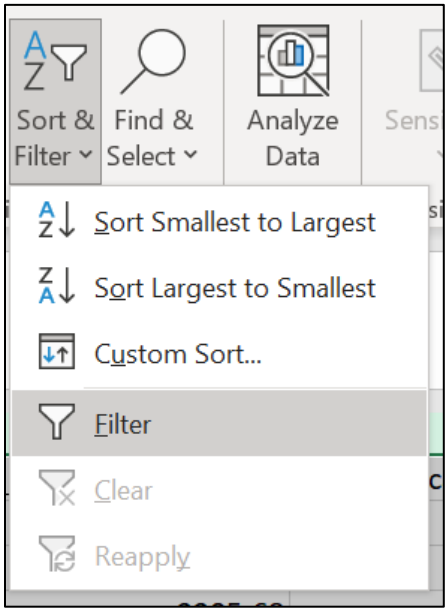

Figure 44) MS Excel's 'Filter' functionality.

Using the filter dropdown that appears in the “Mineralogy_SWIR” column header, deselect “White_Mica” (Figure 45).

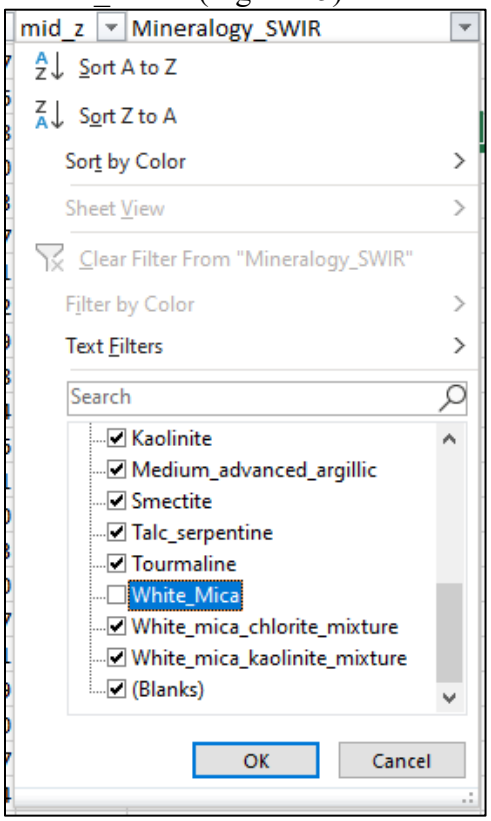

Figure 45) Example of (temporarily) filtering out pure white mica spectra so that the W2200 vectoring scalars can be cleared of values for samples that are NOT purely white mica.

Select all the remaining entries in the three columns that were copy/pasted and erase their contents (right-click and "Clear Contents"). Use the Mineralogy_SWIR filter and turn the white micas back on. These three columns can now be used for vectoring using white mica chemistry. Rename "W2200" to "White_Mica_Composition", "D2200" to "White_Mica_Abundance", and "White_Mica_Crystallinity" to "White_Mica_Crystallinity_filtered".
Repeat this process for the W2250 and D2250 columns, except deselecting "Chlorite", and renaming "W2250" to "Chlorite_Composition" and "D2250" to "Chlorite_Abundance". These may also provide useful vectors in a dataset with abundant chlorite spectra. These four new columns (Figure 46) have been filtered to only the relevant values (pure spectra) and are now valid columns for vectoring.

AI	AJ	AK	AL	AM	AN
Mineralogy_SWIR	White_mica_composition	White_mica_abundance	White_mica_crystallinity	Chlorite_Composition	Chlorite_Abundance
White_mica_chlorite_mixture					
White_mica_chlorite_mixture					
White_mica_kaolinite_mixture					
Smectite					
Chlorite				2262.02	0.098
White_Mica	2201.82	0.38	4.231625835		
White_mica_kaolinite_mixture					
White_mica_chlorite_mixture					
White_Mica	2200.8	0.23	8.778625954		
White_mica_kaolinite_mixture					

Figure 46) Examples of vectoring columns filtered in accordance to the purity of the mineral match for white mica and chlorite, respectively.

In a dataset with abundant alunite, the same composition and abundance columns can be created for the W1485 (Alunite_composition) and D1485 (Alunite_abundance) scalars, but this time deselecting alunite species when they appear in any of Min1, Min2, and Min3.
Once these changes are made, save these results to the same database where the metadata is located, and export the results combined with their spatial information (e.g., coordinates or drillhole collars and depths) and any other data that might be desirable (e.g., corresponding geochemistry results, geological description of samples, etc.). Load this information into a 2D GIS platform (for surface datasets) or 3D platform (for drillhole datasets) and start looking for gradients toward your next discovery!

6. CONCLUSIONS

It is hoped that this walkthrough can aid new users and provide some guidance to experienced users. Aside from the mechanics of working through a dataset, particular attention should be placed on QA-QC considerations, metadata capture, and storage of all products, including metadata, raw spectra in tabular format, and scalar outputs. A far-flung goal of this publication is to enable captured data to be accessed, corrected, and utilized by future workers, fully tapping into the potential of this methodology.

7. REFERENCES

Bedell, R., Crósta, A. P., and Grunsky, E., 2009, Remote sensing and spectral geology, Society of Economic Geologists (SEG).

Bruegge, C. J., Stiegman, A. E., Rainen, R. A., and Springsteen, A. W., 1993, Use of Spectralon as a diffuse reflectance standard for in-flight calibration of earth-orbiting sensors: Optical Engineering, v. 32, p. 805-814.

Chang, Z., Hedenquist, J. W., White, N. C., Cooke, D. R., Roach, M., Deyell, C. L., Garcia, J., Gemmell, J. B., McKnight, S., and Cuison, A. L., 2011, Exploration Tools for Linked Porphyry and Epithermal Deposits: Example from the Mankayan Intrusion-Centered Cu-Au District, Luzon, Philippines*: Economic Geology, v. 106, p. 1365-1398.

Chang, Z., and Yang, Z., 2012, Evaluation of inter-instrument variations among short wavelength infrared (SWIR) devices: Economic Geology, v. 107, p. 1479-1488.

Chi, B., 2022, Github Repository: pytsg, 2022, p. File reader for .tsg files generated by CSIRO's the spectral geologist.

Corbett, G., and Leach, T., 1998, Southwest Pacific Rim Gold-Copper Systems: Structure, Alteration and Mineralization: SEG Special Publication, v. 6.

Crósta, A., 1990, Unveiling Mineralogical Information in Ore Deposits: the Use of Reflectance Spectroscopy for Mineral Exploration in South-America, Brazil.

Cudahy, T. J., Wilson, J., Hewson, R., Linton, P., Harris, P., Sears, M., Okada, K., and Hackwell, J. A., 2001, Mapping porphyry-skarn alteration at Yerington, Nevada, using airborne hyperspectral VNIR-SWIR-TIR imaging data: IGARSS 2001. Scanning the Present and Resolving the Future. Proceedings. IEEE 2001 International Geoscience and Remote Sensing Symposium (Cat. No.01CH37217), 2001.

Duke, E. F., 1994, Near infrared spectra of muscovite, Tschermak substitution, and metamorphic reaction progress: Implications for remote sensing: Geology, v. 22, p. 621-624.

Grove, C., Hook, S. J., and Paylor III, E., 1992, Laboratory reflectance spectra of 160 minerals, 0.4 to 2.5 micrometers, Pasadena, CA: Jet Propulsion Laboratory.

Halley, S., Dilles, J. H., and Tosdahl, R. M., 2015, Footprints: Hydrothermal Alteration and Geochemical Dispersion Around Porphyry Copper Deposits: SEG Newsletter, p. 1-7.

Harraden, C. L., McNulty, B. A., Gregory, M. J., and Lang, J. R., 2013, Shortwave Infrared Spectral Analysis of Hydrothermal Alteration Associated with the Pebble Porphyry Copper-Gold-Molybdenum Deposit, Iliamna, Alaska: Economic Geology, v. 108, p. 483-494.

Hauff, P., 2008, An overview of VIS-NIR-SWIR field spectroscopy as applied to precious metals exploration: Arvada, Colorado: Spectral International Inc, v. 80001, p. 303-403.

Huntington, J., Cudahy, T., Yang, K., Scott, K., Mason, P., Gray, D., Berman, M., Bischof, L., Reston, M., and Mauger, A., 1999, Mineral mapping with field spectroscopy for exploration: Final report: Commonwealth Scientific and Industrial Research Organization, Australia, Exploration and Mining Report, v. 419, p. 35.

Jansen, N., 2016, Good data gives good results: QAQC of NIR data, *in* Perring, S., ed., 2022.

Jansen, N., and Trott, M., 2018, NIR characteristics of porphyry copper deposits, Resources for Future Generations (RFG): Vancouver, British Columbia.

Jones, S., Herrmann, W., and Gemmell, J. B., 2005, Short wavelength infrared spectral characteristics of the HW horizon: Implications for exploration in the Myra Falls volcanic-hosted massive sulfide camp, Vancouver Island, British Columbia, Canada: Economic Geology, v. 100, p. 273-294.

Kerr, A., Rafuse, H., Sparkes, G., Hinchey, J., and Sandeman, H., 2011, Visible/infrared spectroscopy (VIRS) as a research tool in economic geology: background and pilot studies from Newfoundland and Labrador: Geological Survey, Report, v. 11, p. 145-166.

Lampinen, H. M., Laukamp, C., Occhipinti, S. A., Metelka, V., and Spinks, S. C., 2017, Delineating alteration footprints from field and ASTER SWIR spectra, geochemistry, and

gamma-ray spectrometry above regolith-covered base metal deposits—An example from Abra, western Australia: Economic Geology, v. 112, p. 1977-2003.

Laukamp, C., Rodger, A., Legras, M., Lampinen, H., Lau, I. C., Pejcic, B., Stromberg, J., Francis, N., and Ramanaidou, E., 2021, Mineral physicochemistry underlying feature-based extraction of mineral abundance and composition from shortwave, mid and thermal infrared reflectance spectra: Minerals, v. 11, p. 347.

Medina, C. M., Ducart, D. F., Passos, J. S., and de Oliveira, L. R., 2021, Exploration vectoring from the white mica spectral footprint in the atypical auriferous Lavra Velha deposit, San Francisco Craton, Brazil: Ore Geology Reviews, v. 139, p. 104438.

Neal, L. C., Wilkinson, J. J., Mason, P. J., and Chang, Z., 2018, Spectral characteristics of propylitic alteration minerals as a vectoring tool for porphyry copper deposits: Journal of Geochemical Exploration, v. 184, p. 179-198.

Portela, B., Sepp, M. D., Van Ruitenbeek, F. J. A., Hecker, C., and Dilles, J. H., 2021, Using hyperspectral imagery for identification of pyrophyllite-muscovite intergrowths and alunite in the shallow epithermal environment of the Yerington porphyry copper district: Ore Geology Reviews, v. 131, p. 104012.

Russell, J. t., and Farmer, V., 1964, Infra-red spectroscopic study of the dehydration of montmorillonite and saponite: Clay Minerals Bulletin, v. 5, p. 443-464.

Schodlok, M., Whitbourn, L., Huntington, J., Mason, P., Green, A., Berman, M., Coward, D., Connor, P., Wright, W., and Jolivet, M., 2016, HyLogger-3, a visible to shortwave and thermal infrared reflectance spectrometer system for drill core logging: functional description: Australian Journal of Earth Sciences, v. 63, p. 929-940.

Scott, K., and Yang, K., 1997, Spectral reflectance studies of white micas: Australian Mineral Industries Research Association Ltd. Report, v. 439, p. 35.

Scott, K., Yang, K., and Huntington, J., 1998, The application of spectral reflectance studies of chlorites in mineral exploration: North Ryde NSW: CSIRO Exploration & Mining Report, v. 545.

Smith, B., 2016, HyLogger drillhole report for DD90VRB1 'Pear Tree 1', Birrindudu Basin, Northern Territory, HyLogger Data Package 0001, Northern Territory Government.

Swayze, G., Clark, R. N., Kruse, F., Sutley, S., and Gallagher, A., 1992, Ground-truthing AVIRIS mineral mapping at Cuprite, Nevada: JPL, Summaries of the Third Annual JPL Airborne Geoscience Workshop. Volume 1: AVIRIS Workshop, 1992.

Thompson, A. J., Hauff, P. L., and Robitaille, A. J., 1999, Alteration mapping in exploration: application of short-wave infrared (SWIR) spectroscopy: SEG Discovery, p. 1-27.

Trott, M., Munchmeyer, C., and Valenzuela, C., 2018, The Valeriano porphyry copper deposit revisited: 3D geological/geochemical integration and characterization: Resources for Future Generations 2018, Vancouver, Canada, June 2018, 2018.

Trott, M., Sykora, S., Pilsworth, C., and Jansen, N., 2022, Standardization of field-portable short-wave infrared processing for mineral exploration: Explore.

Uribe-Mogollon, C., and Maher, K., 2020, White mica geochemistry: Discriminating between barren and mineralized porphyry systems: Economic Geology, v. 115, p. 325-354.

Van Rossum, G., and Drake Jr, F. L., 1995, Python tutorial, Centrum voor Wiskunde en Informatica Amsterdam, The Netherlands.

Wood, D., and Trott, M., 2017, Porphyry Copper Targeting Under Gravel Cover in Northern Chile, *in* Tschirhart, V., and Thomas, M. D., eds., Exploration '17: Toronto, Ontario, p. 261-274.

APPENDIX A) Metadata / Data Capture Template: "AppendixA_Spectral_Metadata.xlsx".

APPENDIX B) TSG templates and ioGAS color legend: "AppendixB_TSG_templates.zip".

APPENDIX C) Case Studies in the Literature

Numerous studies on the application of SWIR methods to mineral exploration can be found in the public domain and we encourage new users to explore the existing body of work. The following table suggests some (of many) further readings and highlights relevant observations.

Year	Reference	Acquisition Type	Synopsis	Observations
2001	Mapping Porphyry-Skarn Alteration at Yerington, Nevada, Using Airborne Hyperspectral VNIR-SWIR-TIR Imaging Data (Cudahy et al., 2001)	Airborne (HyMap) and Satellite (SEBASS)	Case study at Yerington, Nevada, a well exposed porphyry copper and skarn system. Illustrates the integrated interpretation of airborne and satellite-borne data streams, covering a broad wavelength range (VNIR-SWIR-TIR).	Useful to involve data from beyond the SWIR range (e.g., VNIR and TIR) when possible, and apply higher resolution methods (HyMap) to complement lower resolution methods (SEBASS). In this case mineral zonation is observed in the results (white mica and chlorite chemistry from the SWIR range).
2008	An overview of VIS-NIR-SWIR field spectroscopy as applied to precious metals exploration (Hauff, 2008)	Field Portable	Extremely comprehensive overview of SWIR methods in the context of precious metals exploration. Numerous real-world examples.	Very comprehensive document. Good summary of SWIR active minerals and their relationship with various deposit types.
2013	Shortwave Infrared Spectral Analysis of Hydrothermal Alteration Associated with the Pebble Porphyry Copper-Gold-Molybdenum Deposit, Iliamna, Alaska (Harraden et al., 2013)	Field Portable	SWIR results from acquisition on drill-core at this significant porphyry deposit discussed. Characterization of alteration assemblages and geometry using these methods.	Clear relationship between low W2200 values and higher Au-Cu grades. Case made for the utility of SWIR analysis in constraining 3D geometry.
2015	Footprints: Hydrothermal Alteration and Geochemical Dispersion Around Porphyry Copper Deposits (Halley et al., 2015)	Field Portable	Overview of the results of a consortium project studying zonation around porphyry copper deposits in mineralogical and geochemical terms.	Useful schematic diagrams illustrating mineralogical zonation as well as W2200 contours around an idealized porphyry model. Linkages between this and pathfinder

				geochemistry are explored.
2017	Porphyry Copper Targeting Under Gravel Cover in Northern Chile (Wood and Trott, 2017)	Field Portable	Integration of multiple datasets for exploration below post-mineral cover (including SWIR results from sparse outcrop). Example from northern Chile.	Illustrates fusion of geochemical alteration classification (GER-based) with SWIR results to constrain facies.
2018	NIR Characteristics of Porphyry Copper Deposits (Jansen and Trott, 2018)	Field Portable	Overview of SWIR response for the Haquira East (Peru) and Taca Bajo (Argentina) porphyry deposits, and an anonymous Chilean porphyry prospect. Generalization of some scalar vectors and SWIR-active alteration minerals.	Useful schematic diagrams showing mineralogical zonation with spectral activity in a porphyry scenario. Discusses some potentially misleading scenarios where smectite influence may impact white mica crystallinite and W2200 vectors (Haquira), or isotherm collapse and later overprinting (Taca Taca).
2018	Spectral characteristics of propylitic alteration minerals as a vectoring tool for porphyry copper deposits (Neal et al., 2018)	Field Portable	Study of spectral response of chlorite-bearing rocks from the Batu Hijau porphyry Cu-Au deposit (Indonesia) and systematic variation as a function of distance to system center.	Firmly links the Mg# in chlorite to the W2250 and W2340, and subsequent zonation with regard to the Batu Hijau hydrothermal footprint.
2018	The Valeriano Porphyry Copper Deposit Revisited: 3D Geological/Geochemical Integration and Characterization (Trott et al., 2018)	Field Portable	Integration of SWIR mineralogy with geochemical data to understand system evolution and zonation patterns in the case of the Valeriano porphyry (Chile).	The youngest hydrothermal event is the most prominent. Case made for integration of SWIR results with geochemistry.
2021	Using hyperspectral imagery for identification of pyrophyllite-muscovite intergrowths and alunite in the shallow epithermal environment of the Yerington porphyry copper	Field Portable and Airborne	Detailed study of muscovite replacement of pyrophyllite in the advanced argillic environment in the Yerington district (Nevada), linking textural observations in the laboratory to	Proposal of novel index, the pyrophyllite-muscovite index (PMI) intended to identify areas where pyrophyllite from the advanced argillic assemblage has been

	deposit (Portela et al., 2021)		airborne hyperspectral data.	partially replaced by muscovite.